Tomas Skaar Vadset

Parallel Operation of Synchronous Generators in a DC Grid

Master's thesis in Electric Power Engineering
Supervisor: Mohammad Amin
June 2021

Master's thesis

NTNU
Norwegian University of Science and Technology
Faculty of Information Technology and Electrical Engineering
Department of Electric Power Engineering

NTNU
Norwegian University of
Science and Technology

Tomas Skaar Vadset

Parallel Operation of Synchronous Generators in a DC Grid

Master's thesis in Electric Power Engineering
Supervisor: Mohammad Amin
June 2021

Norwegian University of Science and Technology
Faculty of Information Technology and Electrical Engineering
Department of Electric Power Engineering

NTNU
Norwegian University of
Science and Technology

Preface

This project is a master's thesis undertaken at the Norwegian University of Science and Technology (NTNU) in Trondheim. In autumn, for my specialization project, "Analytical Model for a Synchronous Generator" a model for a single synchronous generator with control elements in an AC grid was created. This master's thesis builds on this specialization project and implements more parts into the components already created. This thesis has been written in cooperation with Vard Electro AS.

The principal part of the master's thesis involves the creation of a simulation model for two synchronous generators in a DC grid. These generators should operate in parallel and be able to operate with variable speed and also use droop control. The objective of the thesis is to ascertain how the system behaves during different operations and to discover why the system behaves as it does. A linear model has also been created to examine the system's stability, but this model is not yet completed and contains some flaws.

I would like to thank my supervisor, Mohammad Amin for always being there to help with answering questions and guiding me throughout my master's thesis and specialization project. I would also like to thank Ulrik Havnsund, Marius Ulla Hatlehol and Martin Skaar Vadset from Vard Electro for providing me with an interesting task for my master's degree project and for their help during this period.

Tennfjord, 2021-06-04

Tomas Skaar Vadset

Abstract

In this master's thesis, a model for two synchronous generators in a DC grid is developed. The model is mainly created in Simulink and consists of two generators with a governor and excitation system each. Each generator is also connected to a six-pulse diode rectifier. The synchronous generator is based on a virtual synchronous generator. The system commences with one generator in a DC grid and later the system is increased to implement two generators. For the excitation system, the AC8B type is used. The governor is a proportional integral (PI) controller and a constant voltage load is used as the load. Droop control for the voltage is also developed for the generators. Tests are conducted with the same droop for both generators and also different droops for each generator. The possibility of variable speed operation is also implemented into the system. Tests are conducted with the droop and variable speed separately and also together to observe how the system behaves. Cases with both generators operating with the same speed and cases in which the generators operate at different speeds are tested. A linear model to examine the stability of one generator with an excitation system and governor is also created. Through testing, it was discovered the system is stable when the droop control and variable speed operate separately, but when they are used together, the system becomes unstable when operating with droop control and variable speed. One of the reasons for this instability, was the PI controller in the governor. After changing the governor, the result became more stable, but the results were still not optimal. The linear model created shows that the system is unstable when the system is stable, and needs further improvements before it is usable.

Sammendrag

I denne masteroppgaven, blir en modell for to synkrongeneratorer i et DC nett utviklet. Modellen er hovedsakelig utviklet i Simulink og består av to generatorer med en governor og excitation system hver. Hver generator er også koblet til en seks-puls diode bro. Synkrongeneratoren er basert på en virtuell synkrongenerator. Systemet starter med en generator i et DC nett før den blir videre utviklet til å simulere to generatorer. Til excitation system er typen AC8B brukt. Til governor er en PI kontroller brukt og en konstant spennings last blir brukt som last. Muligheten til å bruke droop kontroll blir utviklet for generatorene. Tester blir utført både med samme droop og ulik droop for begge generatorene. Muligheten til å operere med variabel hastighet blir også implementert i systemet. Det blir gjort tester med droop kontroll og variable hastighet separat og også samtidig for å se hvordan systemet oppfører seg under disse situasjonene. Det blir testet samme hastighet og ulik hastighet for begge generatorene. En lineær modell for en generator med governor og excitation system blir også laget. Gjennom tester, ble det oppdaget at systemet er stabilit når droop kontroll og variabel hastighet blir brukt hver for seg, mens systemet blir ustabilt når de blir brukt sammen. En av grunnene til at systemet ble ustabilt, var at governoren bruker en PI kontroller. Etter at governoren ble byttet, ble resultatet bedre, men fortsatt ikke optimalt. Lineær modellen som ble utviklet viste at systemet var ustabilt når det burde være stabilt, og trenger derfor videre utvikling før modellen kan brukes.

Contents

List of Figures

1 Introduction

The first attempt at using direct current (DC) on board a ship was in 1880 with the steamship "SS Columbia", where it was used for lighting. In 1922, "HMS Adventure" became the first electric ship, and it used DC motors and generators for propulsion [1]. In recent years, the DC grids on ships have been increasingly developed. With the recent developments in marine operations, DC grids have become a cheap and space-efficient solution for many marine vessels [2].

DC grids have progressed from mostly being used for smaller boats to becoming a viable solution for larger marine vessels as well. The reasons for this viability, depend on what type of ship the DC grid is used for. It is chosen for ferries because it is more cost efficient than an AC grid and it can also be made into a hybrid system by using energy storage such as batteries. Offshore support vessels use DC grids because of the high fault tolerance, along with the previously mentioned benefits [3].

However, one of the main reasons why DC grids have become more common on ships is the possibility they offer of operating the engines with variable speed. Variable speed operation allows the ship to save fuel since the fuel consumption is lower for lower speeds and places less stress on the equipment [3]. When using synchronous generators in parallel in a DC grid aboard marine vessels, it is important that the generators can operate together without creating instabilities.

1.1 Previous work

During the specialization project, an analytical model for a synchronous generator was created using Simulink. This model was compared with a detailed model created using Simscape Electrical. During the project, two cases were simulated; one in which the generator operated under normal circumstances and one in which an additional load was added after a set time. An AC8B excitation system was used for both the detailed and the analytical models. The governor used for the analytical model was a proportional integral derivative (PID) controller, while the detailed model used deGov. This was due to the fact that the signals behave differently in the two models [4].

Through the specialization project, it was discovered that an analytical model provided similar results to a detailed model. However, there was one difference between the results of the two models, which was that the AC voltage for the analytical model was too high. It is important to note when using an analytical model that there are not the same amount of parameters that can be changed compared to a detailed model [4].

A theoretical study was performed during the specialization project, which examined the existing theory concerning synchronous generators, virtual synchronous generators and control systems for generator systems. The symmetrical optimum and modulus optimum tuning methods were used for tuning the excitation system and governor for both analytical and detailed the model. These different theories for the components were further used in the master's thesis [4].

1.2 Problem description

In this project, an analytical model that was created in the specialization project is further developed and tested in a parallel operation for synchronous generators in a DC grid. The following main tasks are undertaken:

- Create a simulation for a model consisting of two synchronous generators with control systems in a DC grid
- Implement droop control in the control system for the generator
- Implement a variable speed operation
- Simulate droop control and variable speed control separate and together
- Examine the simulation results and observe how the different components work separately and together
- Create a detailed model which can be used to verify some cases
- Create a linear model which can be used for stability analysis

1.3 Limitations

The model is limited to two generators with two governors and two excitation systems. The control system is not based on a real model as is the case with the generator. This makes it difficult to compare the analytical model with a proper generator system.

1.4 Software

The software packages used the master's thesis are MATLAB and Simulink. MATLAB is a platform facilitates programming and numeric computations. It uses a language based on scripts. By adding different packages to MATLAB, more possibilities become available [5]. Simulink is one such package. Simulink is simulation and model-based and allows the user to create block diagrams for the system [6]. For this project the Simscape Electrical package from Simulink was used. This package contains finished blocks used for electrical modeling and simulations [7].

1.5 Structure of the report

In this report, Chapter 1 is the introduction to the master's thesis. The system used for the project is shown in Chapter 2. Chapter 3 provides the theoretical background for the master's thesis. The modeling for both the linear and Simulink models is described in Chapter 4. Chapter 5 shows the simulation results for both the Simulink model and the linear model. A discussion of the results is provided in Chapter 6. Chapter 7 describes different aspects of the models that require further improvements. Chapter 8 conclude the master's thesis.

2 System

The system consists of two synchronous generators in parallel with a diode rectifier each, connected to the same bus with a constant voltage load for DC. Each generator has a governor and an excitation system. Variable speed control is implemented for the governor and droop control is implemented for the excitation system. Figure 1 shows a simple drawing of the system used for this project. The generator is a 705V synchronous generator that has a power rate of 2589kVA. For the control system, an AC8B excitation system is used for the voltage control, and a PI controller is used for speed control. This system is much simpler than a real system on board a ship would be, but there are opportunities to expand the system at a later date.

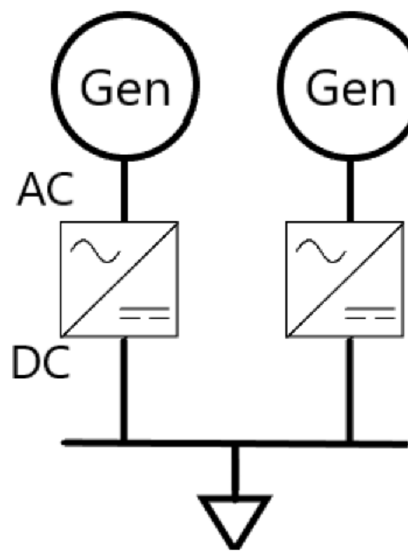

Figure 1: The system used for the project

3 Theory

3.1 Direct current grids on ships

In recent years, low voltage direct current (LVDC) grids have become increasingly common on marine vessels. This widespread use is due to the advantages these grids offer such as space optimization and the ability to operate the engines with variable speeds. By using bidirectional DC-DC converters, it is also possible to use energy storage devices. Another advantage of LVDC grids is that the DC voltage is the only parameter that needs to be considered when connecting more generators. With DC grids, it is possible to reduce the number of transformers and AC components in the system compared to AC grids, which is both space- and cost-efficient. This reduction also results in lower power losses [8]. Figure 2 shows an example of how components can be removed in a DC grid compared to an AC grid.

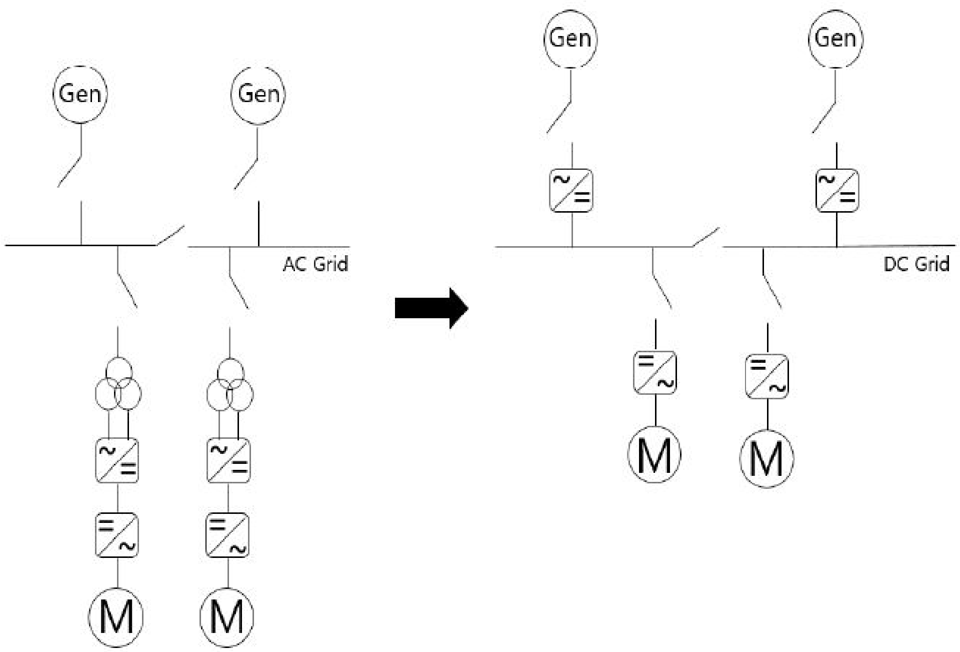

Figure 2: Comparison between AC and DC distribution grid on ships. [9]

In DC systems, there is a difference in how the load sharing is performed compared to AC systems. In an AC system, the excitation system controls the voltage regulation, and the load sharing is controlled using frequency droop by varying the prime mover's speeds. In DC systems, the only parameter that is shared between the two generators, is the DC voltage. There is no need to account for the reactive power and frequency. Only the active power needs to be taken into consideration. The load sharing and the voltage regulation are therefore both controlled by the excitation system [10].

3.2 Direct current droop control

Voltage droop control is the most common control method for load sharing in DC grids. In this project, voltage droop control is central. There is also a possibility of implementing droop speed control for the governor. With droop control, the voltage reference is linearly reduced as the output current increases. This method does not require the generators to communicate with each other, rather; it uses the measured DC voltage. Using the droop control method, it is possible to have one of the generators supply more power than the other. In Equation 1 the reference DC voltage can be observed. This equation is characteristic of the droop controller: V_0 is the no-load reference voltage and δ is the slope that defines the rate of the voltage drop [11]. This means that if the droop constant is 0.1, the power supplied from the generator should be 1pu and the voltage drop for the generator will be 10%.

$$V_{DC}^{*} = V_0 - \delta P_{gen} \tag{1}$$

The parameters V_0 and δ are calculated using the equations 2 and 3. When the two generators share the load,it can be shared 50/50 or one generator can supply more power than the other [12].

$$\delta = \frac{\Delta V_{max}}{P_{max}} \tag{2}$$

$$V_0 = V_{DC,n} + \frac{V_{max}}{2} \tag{3}$$

Figure 3 shows an example of a droop characteristic curve for two generators that are sharing the same load. In this case, the two generators both have a droop of 10% but they have different output voltages. The output voltage for Generator 1 is 1.07pu, while it is 1.03pu for Generator 2. The curve is then drawn using Equation 1. From this curve it can be seen that if the voltage is 1pu with 1pu load, Generator 1 can supply 0.7pu of the load while Generator 2 supplies 0.3pu.

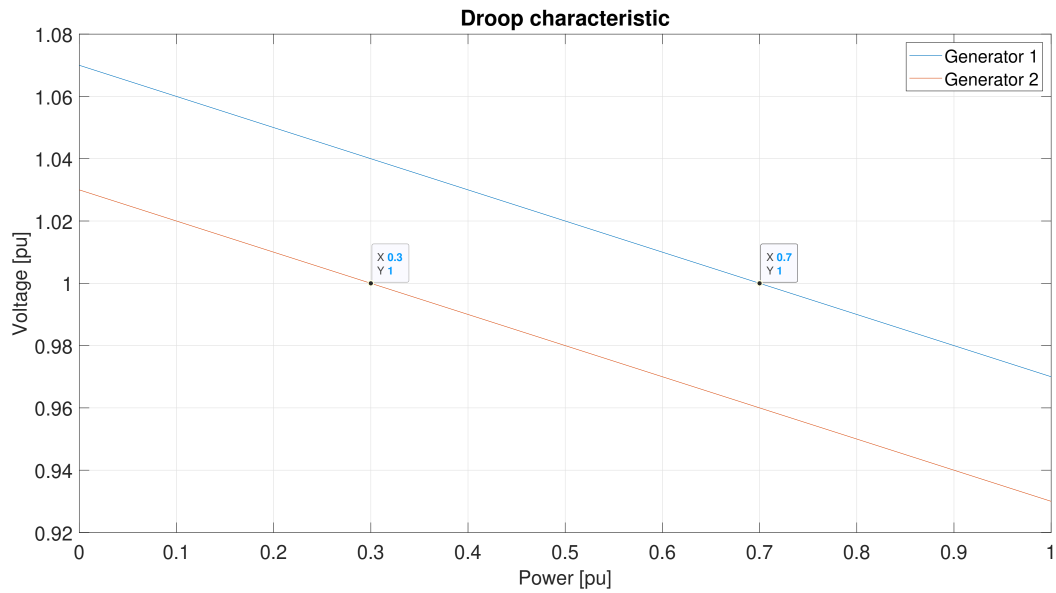

Figure 3: Droop curve for two generators with 10% droop

3.3 Automatic voltage regulator

The automatic voltage regulator (AVR) is an important component of the excitation system. The main principle of the AVR is to turn fluctuating voltage into constant voltage. When the rotating speed of the generator changes, the AVR should keep the voltage constant. This constant voltage prevents equipment from being damaged by too high or low voltage levels [13].

In DC grids, there is the opportunity to operate the engines with variable speed. When the reference voltage is kept constant regardless of the variable speed, over-excitation, which is also refereed to as over-flux, can occur. This can cause damage to equipment and also affect the system. Over-fluxing is a phenomenon that occurs when the flux is over the limit that is permitted for the generator. This can occur when the generator needs to generate the rated voltage with speed below the rated speed and also when the generator generates voltage above the rated voltage with the rated speed [14].

Equation 4 shows the output voltage V_T for the generator, where N is the number of windings on the rotor pole, f is the frequency, and ϕ_m is the rotor flux. The windings are constant, and this means that if the speed is lowered, there is a need to increase the rotor flux to achieve the same rated voltage [14].

$$V_T = 4.44N\phi_m f \tag{4}$$

3.4 Variable speed operation

Variable speed operation of the engine is one of the advantages of using a DC grid. Operating with variable speeds allows the engines to operate more fuel efficiently. This operation cannot be carried out in AC-grids because the generators run at a fixed frequency (50Hz or 60Hz). In AC-grids, there are times when a small generator needs to be added to supply power when the ship is in port. This is often necessary for large ships. With variable speed operation, this is not necessary since the generator can operate at low speed with lower fuel consumption. [15]

By utilizing variable speed operations, it is possible to decrease or increase the speed of the engine depending on the load size. With variable speed operations, it is possible to reduce the fuel consumption by 15% and increase the time between overhauls by 20% [15]. One of the occasions where variable speed operation is useful is when the ship is in a standby phase. For constant speed operation, the fuel consumption is the lowest in a small operating window at approximately 85% of the rated load. By using variable speed operations, this window is increased to 50-100% [16]. Using a load limit curve makes it possible to ascertain at which speed it is optimal to operate. An example of such a curve is illustrated in Figure 4. In this figure, the area inside the blue line is the operating area for the generator, and the red lines show the fuel consumption at different speeds [17].

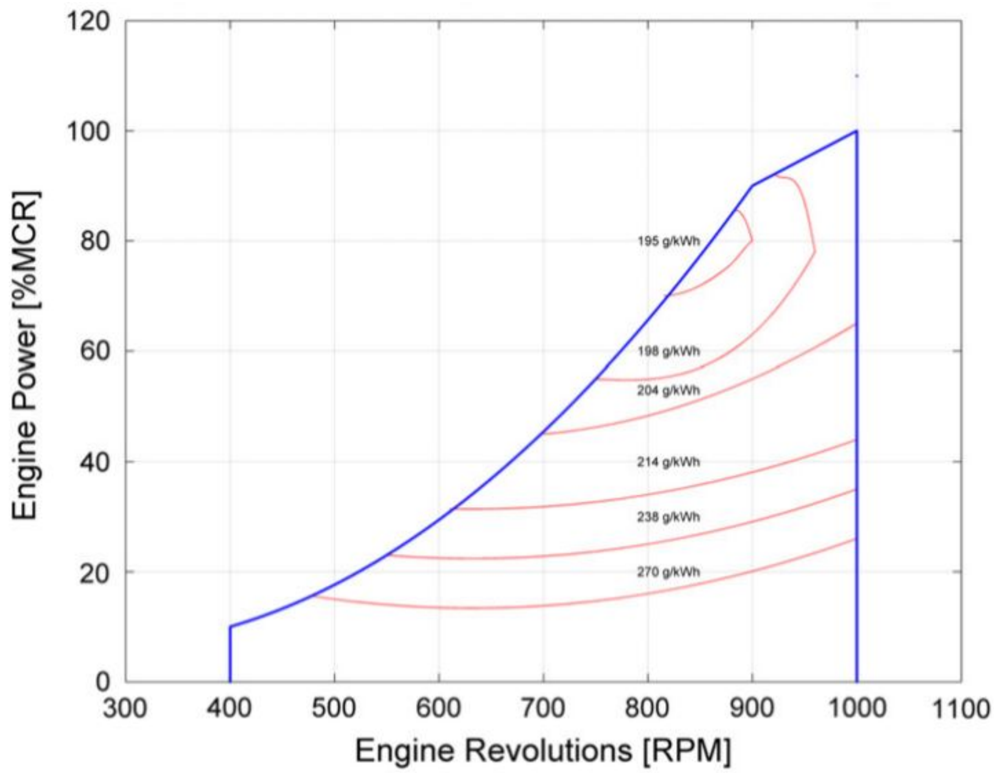

Figure 4: Example of specific fuel consumption of diesel generator engine. [17]

3.5 State space modeling

In state-space modeling, a dynamic model is created to describe a physical system. This model consists of differential equations that describes the behavior of the system. These differential equations are only first order. The goal of state-space modeling is to use the state variables to predict the future behavior of the system. This means that state variables are variables that summarize the history of the system. These state variables are used to create the state vector. Equation 5 shows how a state-space model can be represented. In this case X is the state vector, $\dot{X}$ is the differential state vector, A is the system matrix, B is the input matrix, and U is the input vector [18].

$$\dot{X} = AX + BU \tag{5}$$

3.6 Small-signal stability

The small-signal stability is the ability a system has to maintain synchronism when subjected to a small disturbance. For small disturbances, one way to ascertain whether the system is stable or unstable is to analyze the eigenvalues. The eigenvalues can be calculated; then by using the roots of the eigenvalues, it is possible to see how the system will behave. If the imaginary part of the root is positive, it means that the system is unstable. If the root has no imaginary part, it means that the system is critically stable, and if the imaginary part of the root is negative, it means that the system is stable [19]. The differential equations are represented in the matrix form $\dot{X} = AX$, where X is the state vector, and A is the state matrix. The eigenvalues can then be calculated using Equation 6, where I is the identity matrix, and λ will be the roots of the eigenvalue [20]. [21]

$$det(A - I\lambda) \tag{6}$$

When the roots form a complex conjugate pair, it is possible to calculate the damping ratio. This can be performed using Equation 7. In this case, α is the real part of the root, called the damping coefficient, and Ω is the imaginary part of the root, which is the oscillation frequency [20].

$$\zeta = \frac{-\alpha}{\sqrt{\alpha^2 + \Omega^2}} \tag{7}$$

From Equation 7, it can be observed that with a larger real part of the root, there will also be larger damping for the system. This also means that larger imaginary parts will produce higher oscillations for the system [20].

4 Modeling

4.1 Improvements on the analytical model

The analytical model for the synchronous generator from the specialization project had several problems that needed to be resolved. The main problem was that it did not supply the correct voltage. One of the reasons that the voltage was wrong is that some of the base values used to calculate the per-unit values were incorrect. Rather than using the nominal voltage, which was initially used in the analytical model, the peak voltage should be used. This means that the base value is $705V * \sqrt{2}$. The speed used to calculate some of the variables in the excitation system was not calculated in per-unit values, which will also affect the excitation system.

The output voltage goes through a dq0-transformation before it is used to calculate the terminal voltage. Then the terminal voltage is used in the excitation system. This transformation was created using equations found online, and on calculating the terminal voltage, the result was 1pu regardless, which tells the excitation system that this voltage is acceptable and the excitation system does not alter the voltage. The original dq0-transformation has been changed to a dq0-transformation block from Simulink. This new setup can be seen in Figure 5. A clock from Simulink is used with a gain of $2\pi f$ to get wt. The way in which the dq0-block calculates the voltages can be seen in Equation 8 [22]. These are the same equations that were initially used in the analytical model for the specialization project, but they were created using blocks with MATLAB scripts, which is not the optimal method. Some errors were also made in the script.

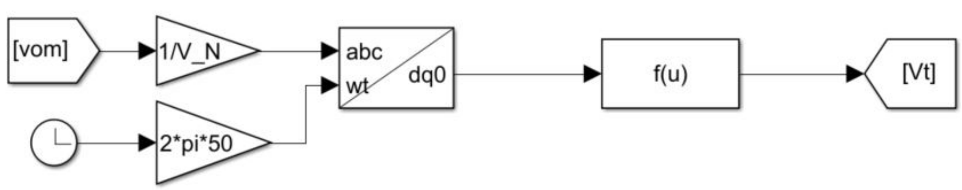

Figure 5: Dq0-transform with Simscape block

$$\begin{bmatrix} V_d \\ V_q \\ V_0 \end{bmatrix} = \frac{2}{3} \begin{bmatrix} \cos\theta & \cos(\theta - \frac{2\pi}{3}) & \cos(\theta + \frac{2\pi}{3}) \\ \sin\theta & \sin(\theta - \frac{2\pi}{3}) & \sin(\theta + \frac{2\pi}{3}) \\ \frac{1}{2} & \frac{1}{2} & \frac{1}{2} \end{bmatrix} \begin{bmatrix} V_a \\ V_b \\ V_c \end{bmatrix} \tag{8}$$

4.2 Analytical model for the system

The total system was created in Simulink and consists of one subsystem for each generator and one subsystem consisting of the rectifier and the dq0-transformation for each generator in the system. There are also subsystems for the control systems for each generator which means that there are two subsystems for the excitation system and two for the governor. The subsystems for the rectifiers are then connected to loads from Simscape Electrical. The complete system for parallel operation can be seen in Figure 6. An resistor capacitor inductor (RCL) element is used in parallel with the load to smooth out the DC voltage.

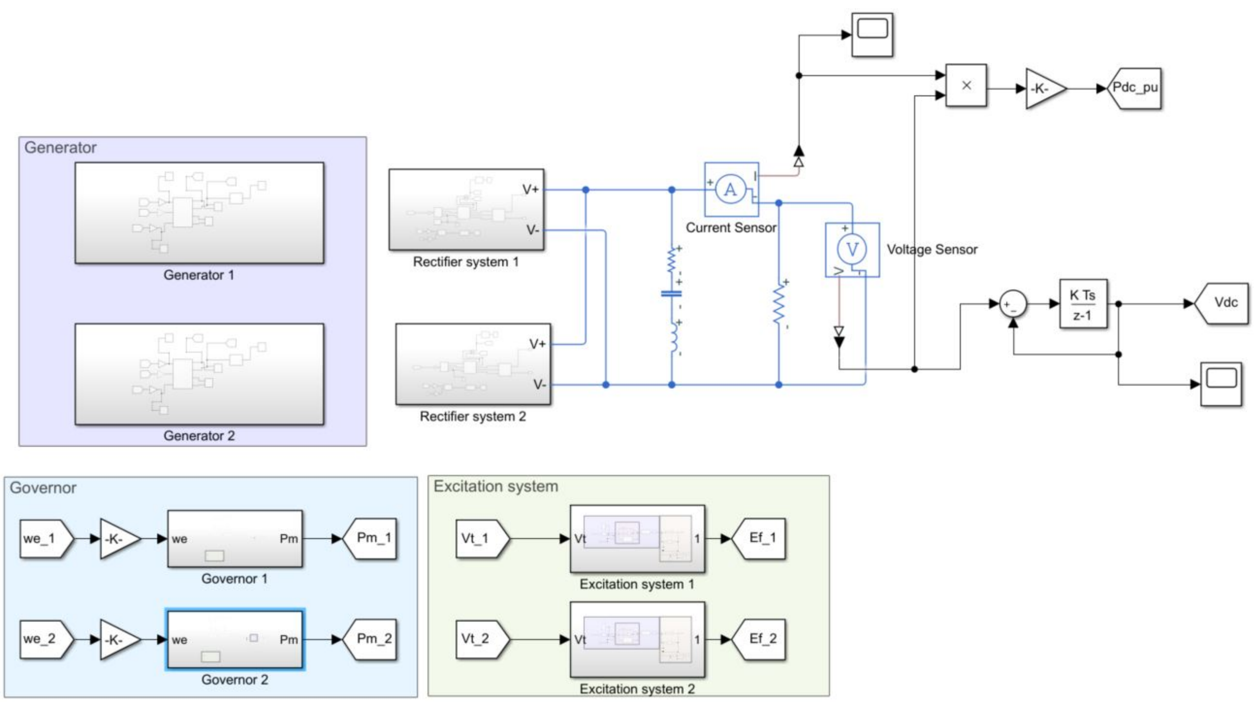

Figure 6: The total system created in Simulink

4.3 Analytical model of the synchronous generator

The subsystem for the generators is comprised of the analytical model of the synchronous generator. This model is based on a synchronverter, which is a type of virtual synchronous generator. Figure 7 depicts the inside of the subsystem called "Generator 1."

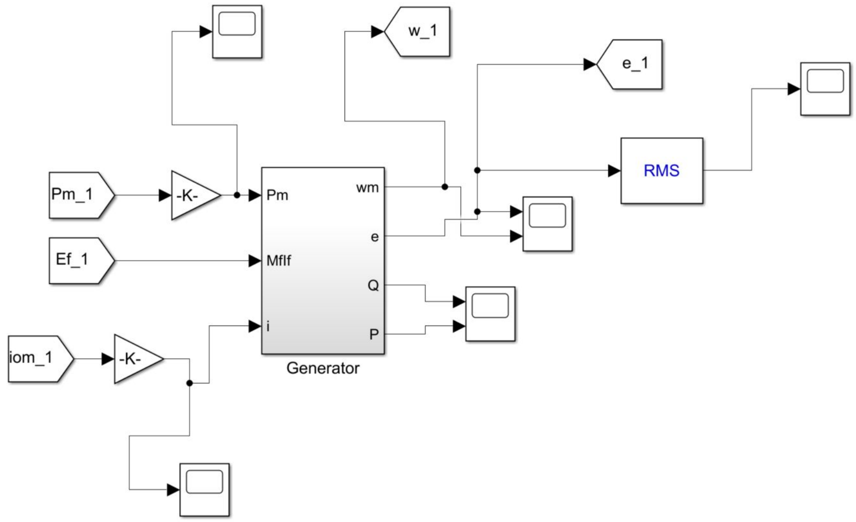

Figure 7: Subsystem for the generator model

The generator model is based on the model from [23] and can be seen in Figure 8. The parameters T_e, e, P and Q are calculated using the equations 9a, 9b, 9c and 9d, where T_e is the electrical torque, e is the voltage, and P and Q are the active and reactive powers. The electrical torque and the feedback from the speed with damping are subtracted from the mechanical torque, which is supplied from the governor. This result, together with the inertia and the integral, is used to calculate the speed. This speed is then used together with the voltage from the excitation system to calculate the electrical torque, the powers and the voltage [23].

$$T_e = -M_f i_f \langle i, \widetilde{\sin}\theta \rangle \tag{9a}$$

$$e = \dot{\theta} M_f i_f \widetilde{\sin}\theta \tag{9b}$$

$$P = \dot{\theta} M_f i_f \langle i, \widetilde{\sin}\theta \rangle \tag{9c}$$

$$Q = -\dot{\theta} M_f i_f \langle i, \widetilde{\cos}\theta \rangle \tag{9d}$$

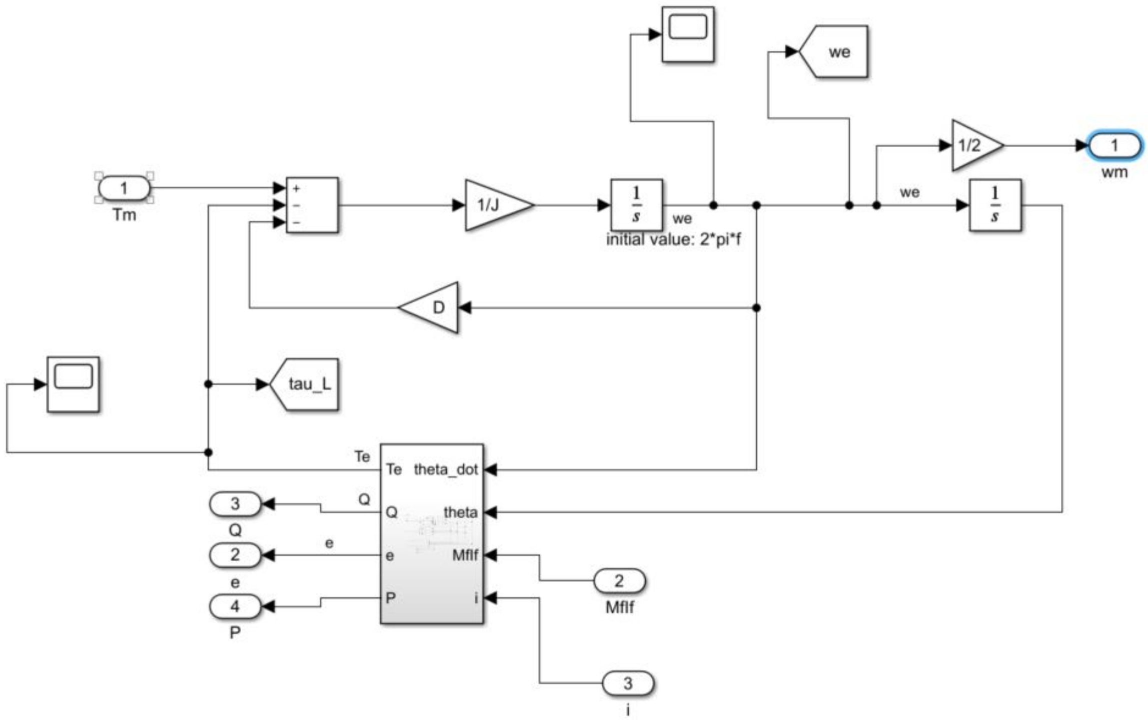

Figure 8: Generator model [4]

4.4 Rectifier subsystem

The subsystem for the rectifier part of the system consists of the rectifier and also the dq0-transformation for the system. The variable e_1 is the voltage that is sent from the generator model in Figure 7. The rectifier system can be seen in Figure 9. A six-pulse uncontrolled diode rectifier was used for the project.

The system uses simple diode rectifiers; therefore, these were not modeled from the beginning. Blocks from Simscape Electrical were used. The parameters for this block were the default ones, as this block is only intended to transform the voltage from AC to DC without any set value. Since it is a normal diode rectifier, the DC voltage should be $\approx 1.35 \cdot V_{AC}$. Consequently, the DC voltage should be 951.75V. There was also the possibility of operating with a six pulse thyristor rectifier, but the diode rectifier was chosen for this project. Some advantages of using diodes rather than thyristor rectifiers are that they do not require an external trigger as the thyristors do, and they are cheaper and occupy less space. The disadvantages of diodes are that they have worse power handling ability and lower operating voltages, but neither of these were issues for this project. Another disadvantage of diode rectifiers; is that they are not controllable. This lack of control was also not an issue for this project. [24]

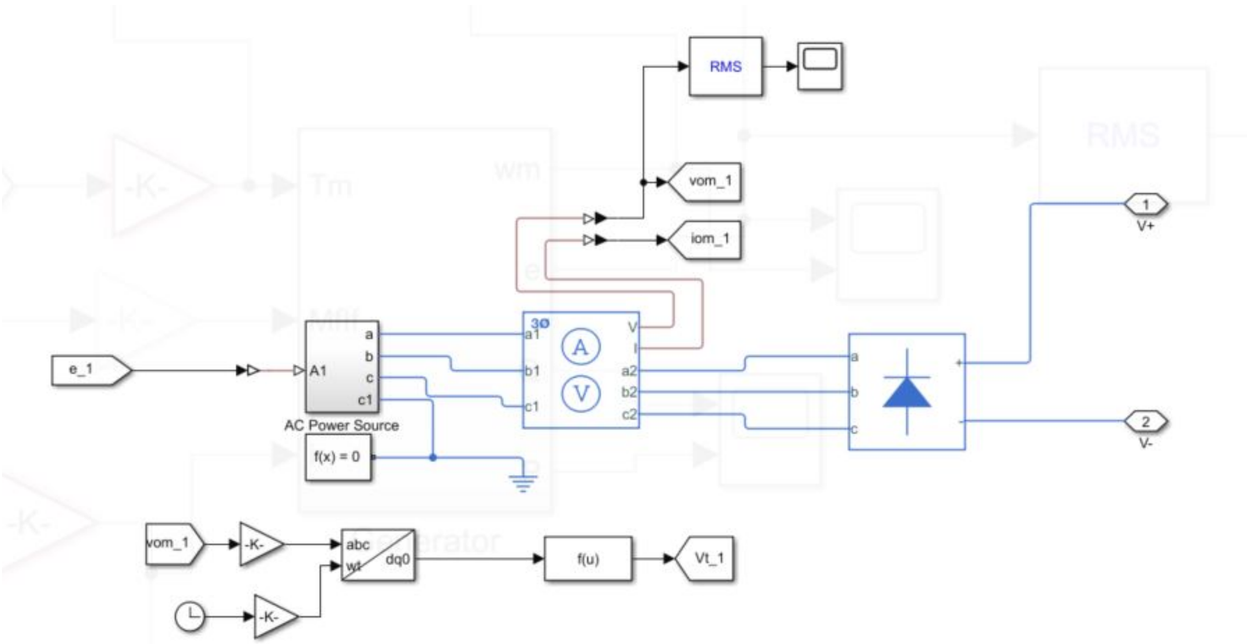

Figure 9: Subsystem for the diode rectifier

4.5 Excitation system

The variable for the voltage is V_{t1} after it is transformed into dq0-components and used to calculate the peak value through the function block. This voltage is then be sent into the AC8B excitation system, which is used to decide the field voltage that will be supplied to the generator. This field voltage is the variable E_{f1}, which can be seen in Figure 10 of the excitation system and also in Figure 7 of the analytical model. The values for the excitation system were obtained using symmetrical optimum, modulus optimum and previous projects [25] [26] [4].

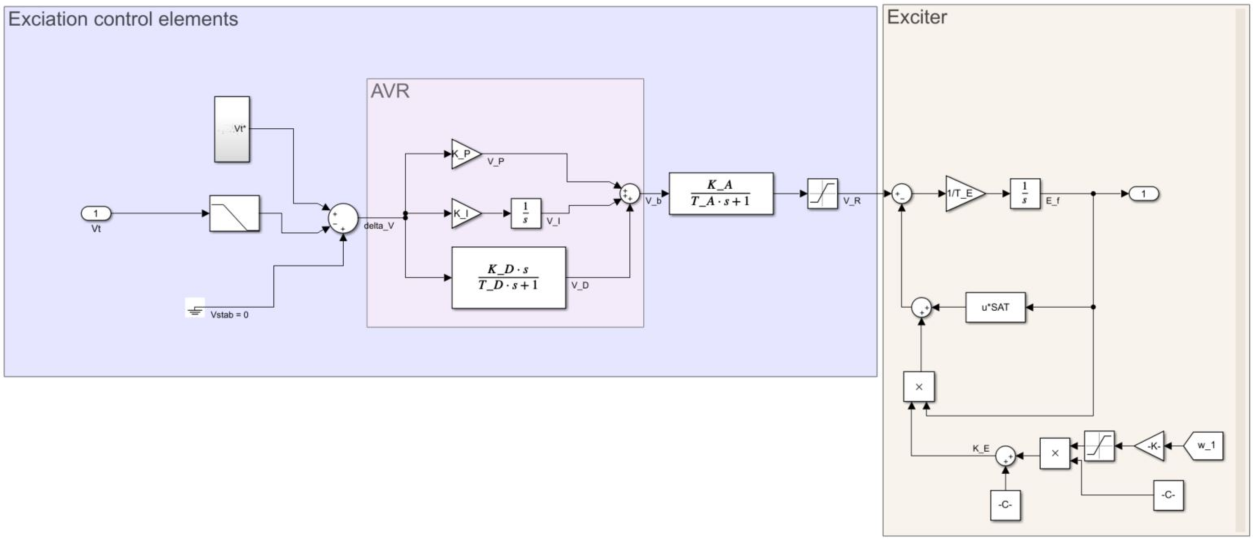

Figure 10: AC8B excitation system

4.6 Governor

In the subsystem for the generator in Figure 7, the variable w_{e1} is calculated and then sent into the governor in Figure 11 as seen in Figure 6. Here the actual speed is compared with the reference speed. The offset is then sent into a PI controller, which transmits how much torque or power the generator should be supplied with. This is the variable P_m, which can be seen in Figure 6 and 7. This is the same variable as T_m in Figure 8.

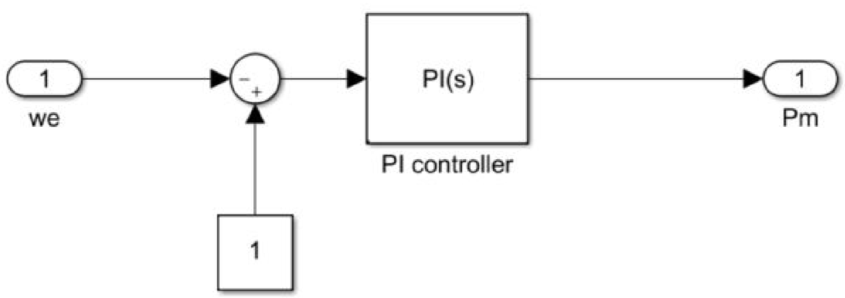

Figure 11: Governor subsystem

Another governor model was also used for a few simulations to observe how it affected the system. This governor was a finished block from Simulink and can be seen in 12. This block does not have a PI controller, unlike the other governor model used, and this is the reason that this block was used as a comparison in some results. By using this block, it is possible to ascertain how the PI controller affects the stability of the system. In this case, the offset between the speed and reference speed is used with the droop to achieve the actual load, which is then compared to the reference load. This offset is then fed into the gain with the time constant T_G which is the governor time constant. In this case, this time constant is 0.2s There is also feedback in the governor.

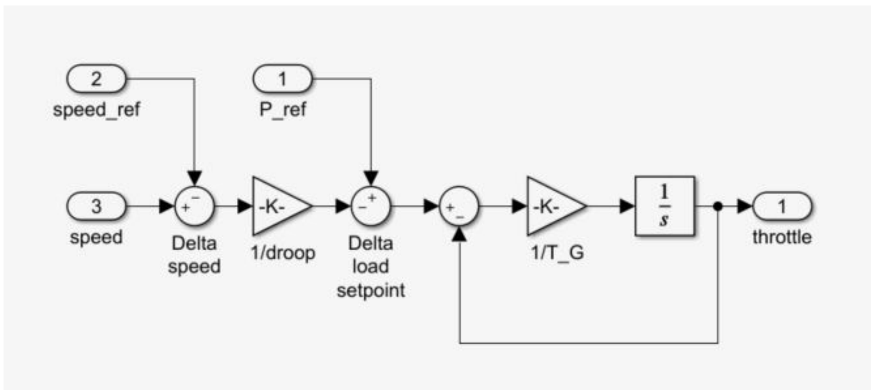

Figure 12: Governor block from Simulink

4.7 Droop control

Originally in the excitation system, a reference value of 1pu was used. This value works for operation with only one generator, but with two generators, droop control is needed to prevent both generators from providing too much power and overloading the load. The setup which was used for the droop at the beginning of the project can be seen in Figure 13. In this case, the DC no-load reference voltage is 1.02pu. The measured DC voltage and the power multiplied by the droop constant of 0.05 are subtracted from the no-load reference value similar to Equation 1. The AC reference value is then added to this value, and a saturation block is used to prevent the value from becoming too high. This provides the variable V_{t1}, which is the reference value for the excitation system.

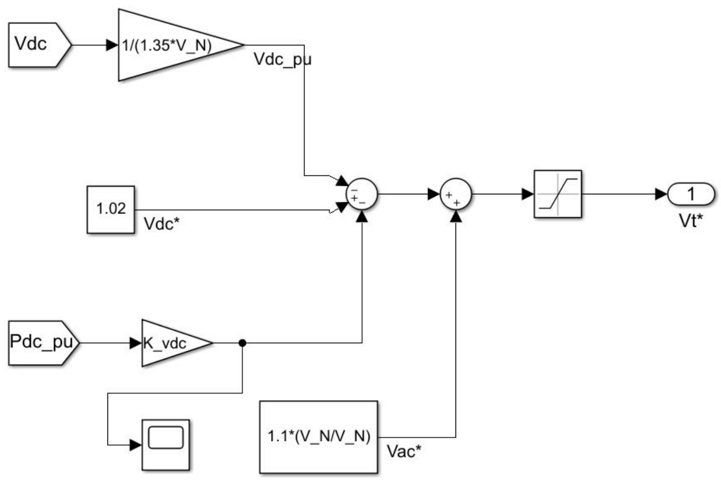

Figure 13: Droop control

The model for droop control in Figure 13 was located in other projects and therefore assumed to be appropriate to use. During the simulations, it was noticed that all the cases with droop control had some commonalities. The DC voltage and power was always quite a bit higher than it should have been. Through testing, it could be observed that the value reference value given by the droop controller was approximately 1.2pu when it stabilized. This means that the droop controller told the excitation system that the desired voltage was higher than it really was, which resulted in high DC voltage and power being supplied. Tests were conducted using the saturation block to prevent the reference value from exceeding 1pu, but this led to the droop controller no longer working and was essentially the same as using a constant block with 1pu.

To fix the high DC voltage and power being supplied, another model was used for the droop controller. This new model is just Equation 1 and can be seen in Figure 14. Figure 14 is from one of the tests where the droop constant was set to 10%, which is the reason the gain was 0.1. The droop controller calculates the difference between the set DC reference and the power multiplied with the droop constant. By using this model, the results were more similar to the expected values.

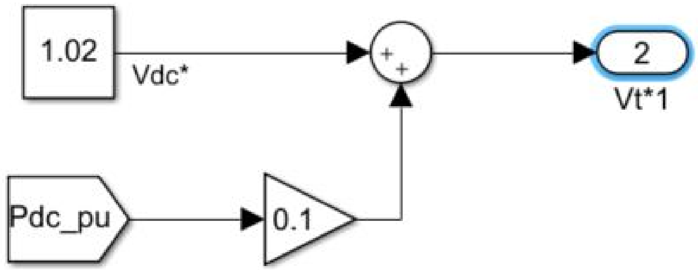

Figure 14: New droop controller

4.8 Load change

Another resistor was added in parallel with the original load to simulate a change in the load. This arrangement can be seen in Figure 15. In this case, a switch was used to connect the resistor to the system after a chosen time. The resistor added to the system had a value of 1Ω. This provided a total resistance of 0.29Ω, which supplied a load of 3118kW after the load change.

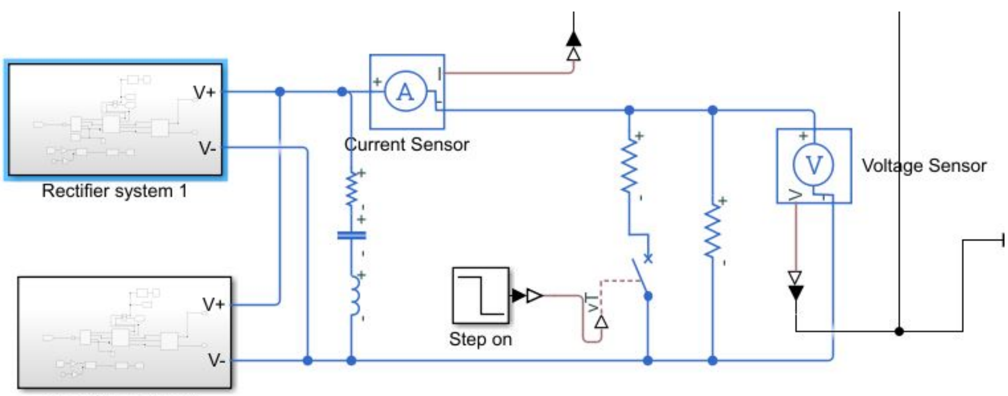

Figure 15: Implementation of load change in Simulink

4.9 Variable speed operation

For this project, two different cases for variable speed operation were simulated. Both cases had the same load change as previously mentioned. The first case involved both generators operating at the same speed, which meant that each cylinder should have an output of $3118kW/18 = 173.26kW$. The load limit curve indicates that it is possible to operate at speeds between 900 and 1000rpm. If the generators operate at a speed of 1000rpm, the fuel consumption per cylinder will be 8000kJ/kWh, while at 900rpm, it will be 7760kJ/kWh. This means that, economically, it will be best to operate at 900rpm after the load change. The total fuel consumption at 1000rpm is 144000kJ/kWh, while at 900rpm, it is 139680kJ/kWh.

To create this variable speed controller, the constant of 1 for the reference speed in Figure 11 was switched out with the subsystem seen in Figure 16. In this case, the power from the generator is first calculated to per-unit values before it is sent into a lookup table. In the table, there are two parameters: the first is the power sent into the table. Then a speed in revolutions per minute (RPM) is sent out depending on the power sent in. This speed is then calculated into per unit value and then used as the new reference speed for the different powers. The values used in the lookup table can be seen in Table 1. A speed curve can also be plotted to demonstrate how the speed will change with the power. This curve can be seen in Figure 17. Looking at this curve it can be observed that if the power supplied by the generator is 0.14pu, the reference speed will be set as 0.6pu, and the speed will be adjusted accordingly and end up at 600RPM.

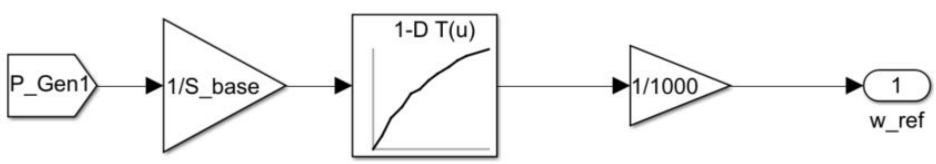

Figure 16: Subsystem for getting reference speed during variable speed operation

Table 1: Lookup table used for variable speed operation

Speed [RPM]	**Power [pu]**
600	0.14
650	0.21
725	0.28
770	0.35
820	0.42
840	0.49
875	0.56
900	0.63
925	0.7
950	0.77
975	0.83
1000	1

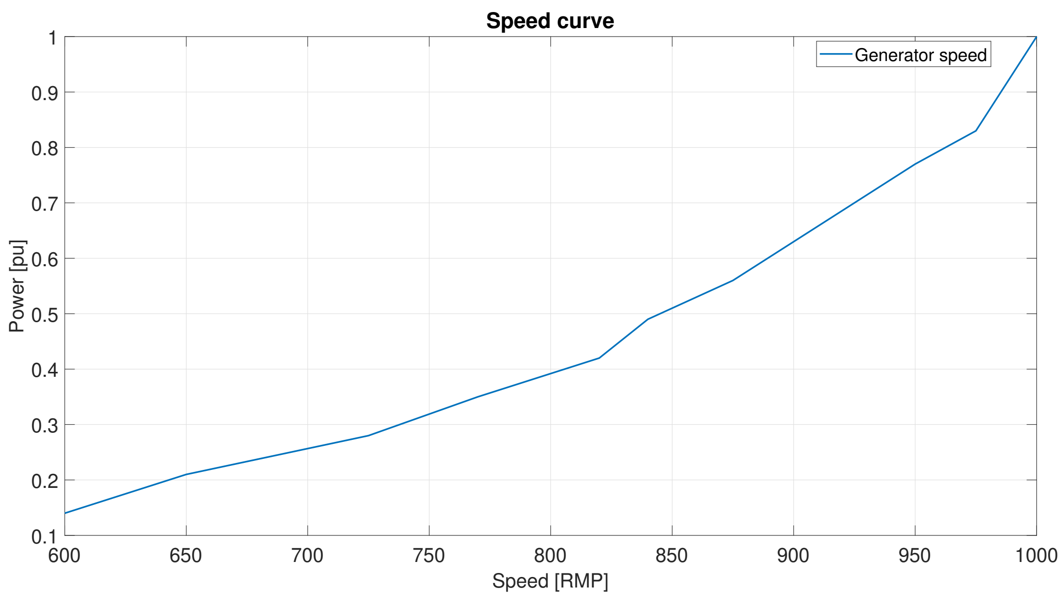

Figure 17: Speed curve dependent on power

In the second case, the two generators will operate at different speeds. One generator will operate at maximum capacity, while the other generator will supply the rest of the required power. The load limit curve indicates, that the maximum output possible from each cylinder is 265kW at a speed of 1000rpm, which gives a total power of 2385kW for the generator. This reading means that the other generator needs to supply $3118kW - 2385kW = 733kW$, which gives 81.44kW per cylinder. At 81.44kW, there is a much wider spectrum of speed in which it can operate, but the speed of 750rpm was chosen because this results in the smallest energy consumption of 8350kJ/kWh per cylinder. The energy consumption for the first generator is 7400kJ/kWh per cylinder. This results in a total energy consumption of 141750kJ/kWh. The droop characteristics need to be changed to implement this variable-speed operation. Previously, both generators had the same droop, which means they operate at the same speed and supplied the same power.

For the case before the load change, the load is 2261kW. If it is desired that Generator 2 supplies the most power, the droop constant can be set lower, for example, at 0.04. This will mean that Generator 2 should supply the most power. In addition, it should also be possible for Generator 2 to supply all the power considering that the load is below the maximum power for the generators. With a droop of 4% and a load of 0.87pu, the voltage change is calculated at 0.0348pu using Equation 2.

4.10 Linearized equivalent model for synchronous generator

The linear model was inspired by the model in [27], [28] and [29]. The values for the constants D_δ, K_2, K_3, K_6 and $K_{E'}$ were all taken from this model.

The synchronous generator has four state variables, which means that it is a fourth-order model [20] [21]. The state variables are $\Delta\dot{\omega}_s$, $\dot{\delta}$, $\dot{E}_q$ and $\dot{V}_g$. The differential equations are derived from one electrical part and one mechanical part for the generator. These parts can be seen in Figure 18.

The mechanical part of the generator has the two state variables $\Delta\dot{\omega}_s$ and $\dot{\delta}$. First, the differential equation for $\Delta\dot{\omega}_s$ is determined. In this case, P_m represents the result from the PI controller, which is shown later; D, D_δ, K_2, K_3, K_6, $K_{E'}$ and M are all constants; K_3 and K_2 are the field winding linearization constants; and K_6 is the armature winding linearization constant. D_δ is a linearization constant. D is the electric damping for the machine, and $K_{E'}$ is the linearization constant for synchronizing power. The differential Equation for $\Delta\dot{\omega}_s$ is shown in equation 10.

$$\Delta\omega = \frac{1}{sM}(P_m - K_{E'} - D_\delta E_q - D\Delta\omega_s)$$

$$s\Delta\omega = \frac{1}{M}(P_m - K_{E'}\delta - D_\delta E_q - D\Delta\omega_s)$$

$$\frac{d\Delta\omega_s}{dt} = \frac{1}{M}(P_m - K_{E'}\delta - D_\delta E_q - D\Delta\omega_s) \tag{10}$$

δ is just $\Delta\omega_s$ integrated, which gives the differential equation for $\dot{\delta}$ is seen in Equation 11.

$$\delta = \frac{\Delta\omega_s}{s}$$

$$s\delta = \Delta\omega_s$$

$$\frac{d\delta}{dt} = \Delta\omega_s \tag{11}$$

The electrical part of the generator also has two state variables. These are E_q and V_g. The variable E_f is a state variable for the excitation system and is derived later in this section. The differential equation for $\dot{E}_q$ can be seen in Equation 12.

$$E_q = \frac{K_3}{1 + T'_{d0}K_3 s}(E_f - \Delta\delta K_2)$$

$$E_q(1 + T'_{d0}K_3 s) = E_f - \Delta\delta K_2$$

$$E_q + E_q T'_{d0}K_3 s) = E_f - \Delta\delta K_2$$

$$\frac{dE_q}{dt} = \frac{1}{T'_{d0}}(E_f - \Delta\delta K_2 - \frac{E_q}{K_3}) \tag{12}$$

The differential equation for V_g can be seen in Equation 13.

$$V_g = \frac{K_3 K_6}{1 + T'_{d0} K_3 s}(E_f - \Delta\delta K_2)$$

$$V_g(1 + T'_{d0} K_3 s) = K_3 K_6 (E_f - \Delta\delta K_2)$$

$$V_g + V_g T'_{d0} K_3 s = K_3 K_6 (E_f - \Delta\delta K_2)$$

$$\frac{dV_g}{dt} = \frac{1}{T'_{d0}}[(E_f - \Delta\delta K_2)K_6 - \frac{V_g}{K_3}] \tag{13}$$

All the differential equations for these state variables can be seen in 14. The values for the direct- and quadrature short-circuit time constants for the transient and sub-transient state can be seen in Table 2 in the appendix.

$$\begin{bmatrix} \Delta\dot{\omega}_s \\ \dot{\delta} \\ \dot{E}_q \\ \dot{V}_g \end{bmatrix} = \begin{bmatrix} \frac{1}{M}(P_m - K_{E'}\delta - D_\delta E_q - D\Delta\omega_s) \\ \Delta\omega_s \\ \frac{1}{T'_{d0}}(E_f - \Delta\delta K_2 - \frac{E_q}{K_3}) \\ \frac{1}{T'_{d0}}[(E_f - \Delta\delta K_2)K_6 - \frac{V_g}{K_3}] \end{bmatrix} \tag{14}$$

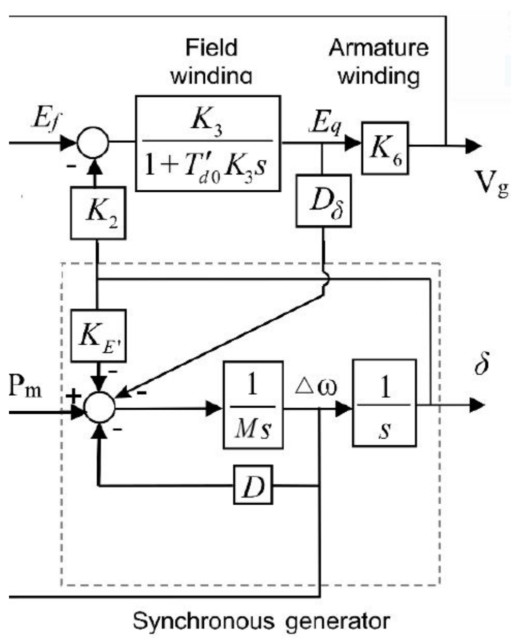

Figure 18: Block diagram with state variables for the synchronous generator

4.11 Linearized equivalent model for excitation system

The excitation system used in the model is of the AC8B type, and the block diagram for the excitation system can be seen in 19 [30]. There are four state variables for the excitation system: $\dot{E}_f$, $\dot{V}_R$, $\dot{V}_{IR}$ and $\dot{V}_{DR2}$ [27] [28] [29]. The values for the different parameters can be seen in Table 3.

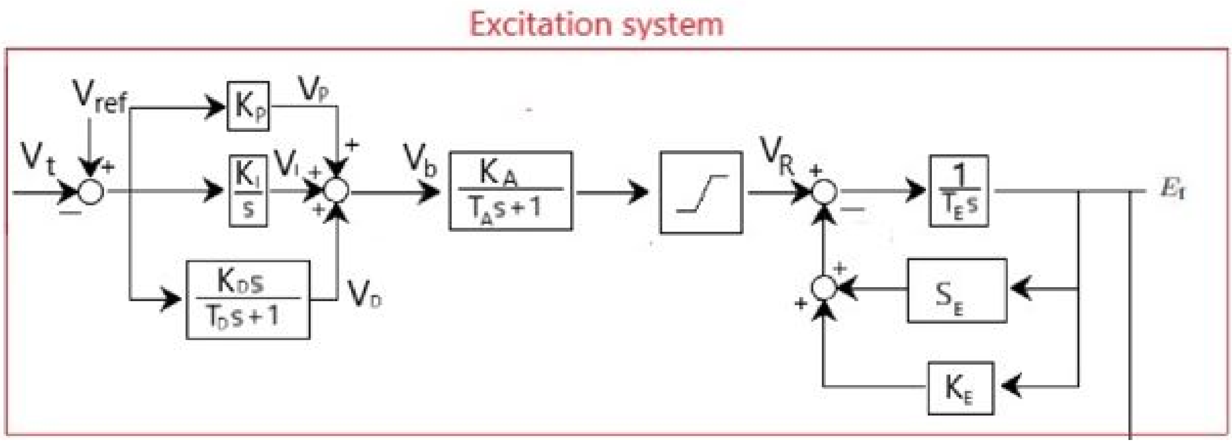

Figure 19: Block diagram for the AC8B excitation system

The state variable $\dot{E}_f$ is the state variable which is also used in the electrical part for generator model. This state variable has the differential equation seen in Equation 15.

$$E_f = \frac{1}{T_E s}[V_R - (S_E + K_E)E_f]$$

$$sE_f = \frac{1}{T_E}[V_R - (S_E + K_E)E_f]$$

$$\frac{dE_f}{dt} = \frac{1}{T_E}[V_R - (S_E + K_E)E_f] \tag{15}$$

The state variable $\dot{V}_R$ is the voltage out from the regulator. The differential equation can be seen in Equation 16.

$$V_R = \frac{K_A V_b}{T_A s + 1}$$

$$V_R(T_A s + 1) = K_A V_b$$

$$V_R T_A s + V_R = K_A V_b$$

$$V_R s = \frac{1}{T_A}(K_A V_b - V_R)$$

$$\frac{dV_R}{dt} = 1/T_A(K_A V_b - V_R) \tag{16}$$

The variable V_b is a variable for the result from the PID regulator. The equation for this variable can be seen in Equation 17.

$$V_b = K_{PR}(V_{ref} - V_t) + \frac{K_{IR}}{s}(V_{ref} - V_t) + \frac{K_{DR}s}{T_{DR}s+1}(V_{ref} - V_t)$$

$$V_b = K_{PR}(V_{ref} - V_t) + K_{IR}V_{IR} + K_{DR}V_{DR} \tag{17}$$

For the AVR, there are two state variables created, these are $\dot{V}_{IR}$ and $\dot{V}_{DR2}$. The differential equation for $\dot{V}_{IR}$ is shown in Equation 18.

$$V_{IR} = \frac{1}{s}(V_{ref} - V_t)$$

$$\frac{dV_{IR}}{dt} = V_{ref} - V_t \tag{18}$$

The state variable for the derivative part of the AVR comes from Equation 19.

$$V_{DR} = \frac{s}{T_D s + 1}(V_{ref} - V_t) \tag{19}$$

$$V_{DR}T_{DR} + V_{DR}\frac{1}{s} = V_{ref} - V_t$$

A new variable V_{DR2} is created as a state variable. This can be seen in Equation 20. This also gives the differential equation for $\dot{V}_{DR2}$ in Equation 21.

$$V_{DR2} = \frac{1}{s}V_{DR} \tag{20}$$

$$\frac{dV_{DR2}}{dt} = V_{DR} \tag{21}$$

Now using V_{DR2} the equations will be

$$V_{DR} = \frac{1}{T_{DR}}[(V_{ref} - V_t) - V_{DR2} \tag{22}$$

Now switching out V_{DR} in Equation 21 with Equation 22 the result will be Equation 23.

$$\frac{dV_{DR2}}{dt} = \frac{1}{T_{DR}}[(V_{ref} - V_t) - V_{DR2}] \tag{23}$$

Switching out V_{DR} in Equation 17, the new equation becomes Equation 24.

$$V_b = K_{PR}(V_{ref} - V_t) + K_{IR}V_{IR} + K_{DR}\frac{1}{T_{DR}}[(V_{ref} - V_t - V_{DR2}] \tag{24}$$

All the state variables for the excitation system can be seen in the matrix in 25.

$$\begin{bmatrix} \dot{E}_f \\ \dot{V}_R \\ \dot{V}_{IR} \\ \dot{V}_{DR2} \end{bmatrix} = \begin{bmatrix} \frac{1}{T_e}[V_R - (S_E + K_E)E_f] \\ \frac{1}{T_a}(K_a V_b - V_R) \\ V_{ref} - V_t \\ \frac{1}{T_{DR}}[(V_{ref} - V_t) - V_{DR2}] \end{bmatrix} \tag{25}$$

4.12 Linearized equivalent model for governor

The governor used for the analytical model was a PI controller, which can be observed in Figure 20. This gives one state variable $\dot{\omega}_{IG}$ for the integrator part of the PI controller. From the block diagram, it is also possible to see the equation for P_m, which is an input variable for the mechanical part of the generator. This can be seen in Equation 26. The values used for the governor can be seen in Table 4 in the appendix.

$$P_m = K_{PG}(\omega_{ref} - \omega) + \frac{K_{IG}}{s}(\omega_{ref} - \omega) \tag{26}$$

The differential equation for $\dot{\omega}_{IG}$ can be seen in Equation 27.

$$\omega_{IG} = \frac{1}{s}(\omega_{ref} - \omega)$$

$$\frac{d\omega_{IG}}{dt} = \omega_{ref} - \omega_t \tag{27}$$

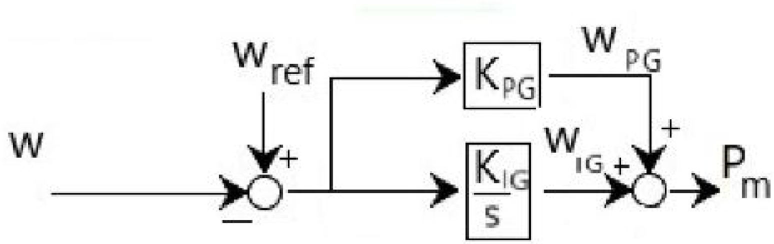

Figure 20: Block diagram for governor

4.13 Linearized equivalent model for the whole system

From the previous three sections, it can be seen that the whole system has a total of nine state variables. These are $\Delta\dot{\omega}_s$, $\dot{\delta}$, $\dot{E}'_q$, $\dot{V}_g$, $\dot{E}_f$, $\dot{V}_R$, $\dot{V}_{IR}$, $\dot{V}_{DR2}$ and $\dot{\omega}_{IG}$. The differential equations from 14, 25 and 27 is put together into one state matrix for the whole system as seen in the state vector in 28. The input variables can be seen in the vector in 29. The time constants for the generator come from the data sheet for the generator, while the gain and time constants for the governor and excitation system has been found using tuning methods and manual tuning [4]. The total block diagram for the generator with control structures can be observed in Figure 21.

$$\begin{bmatrix} \Delta\dot{\omega}_s \\ \dot{\delta} \\ \dot{E}_q \\ \dot{V}_g \\ \dot{E}_f \\ \dot{V}_R \\ \dot{V}_{IR} \\ \dot{V}_{DR2} \\ \dot{\omega_{IG}} \end{bmatrix} = \begin{bmatrix} \frac{1}{M}(P_m - K_{E'}\delta - D_\delta E_q - D\Delta\omega_s) \\ \Delta\omega_s \\ \frac{1}{T'_{d0}}(E_f - \Delta\delta K_2 - \frac{E_q}{K_3}) \\ \frac{1}{T'_{d0}}[(E_f - \Delta\delta K_2)K_6 - \frac{V_g}{T'_{d0}K_3}] \\ \frac{1}{T_e}[V_R - (S_E + K_E)E_f] \\ \frac{1}{T_a}(K_a V_b - V_R) \\ V_{ref} - V_t \\ \frac{1}{T_{DR}}[(V_{ref} - V_t) - V_{DR2}] \\ \omega_{ref} - \omega_t \end{bmatrix} \tag{28}$$

$$U = \begin{bmatrix} \omega_{ref} \\ V_{ref} \end{bmatrix} \tag{29}$$

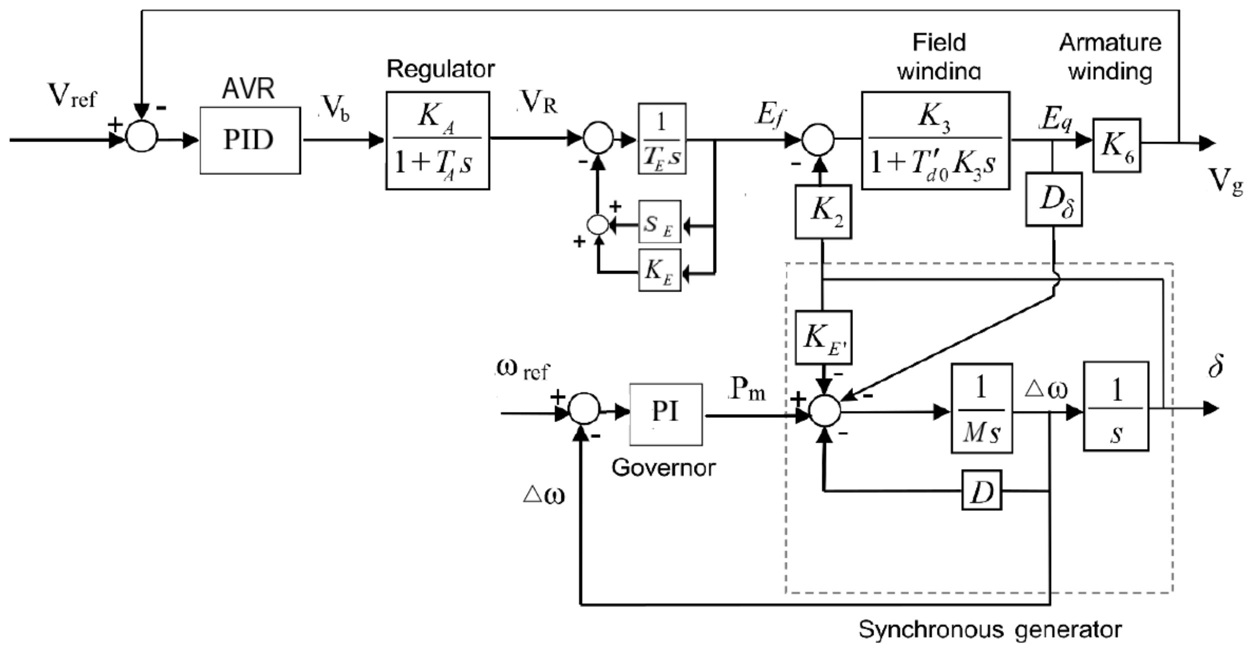

Figure 21: Block diagram for generator, governor and excitation system

4.14 Detailed model

A detailed model using blocks from Simscape Electrical was created in the specialization project [4]. This model is also further used in this project to verify the results and compare how closely the results from the analytical model resemble the detailed model. If there are anomalies with the simulation results for the analytical model, the detailed model can be used to ascertain whether there are faults with the analytical model or other parts of the models.

This system can be seen in Figure 22. This system consists of two of the same type of excitation system as the analytical model and two governors of the deGov type. The generators have the exact same values as do the two diode rectifiers. The load is a resistor which represents a constant voltage load.

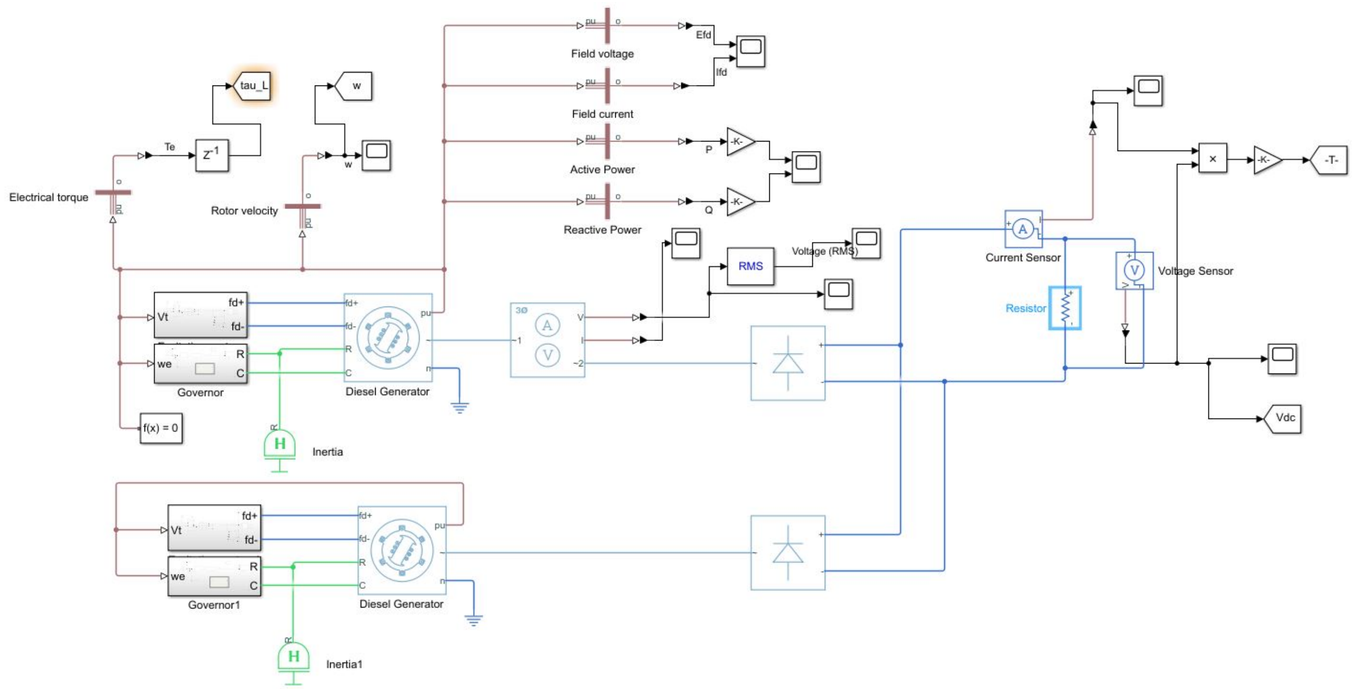

Figure 22: Simulink model for parallel operation with detailed model.

5 Simulation results

5.1 Simulink model

5.1.1 Analytical model improvements

The previous section mentioned that the analytical model for the synchronous generator needed to be changed to achieve the desired voltage. Figure 23 shows the comparison between the model before and after the improvements previously mentioned. It can be observed that the voltage is now 704.9V, which is excellent considering the nominal voltage is 705V. This voltage is much better when compared to the 887.6V from earlier. There is also less noise for the signal, but it can also be observed that the system is now much slower than it was during the specialization project. It now takes almost 20 seconds before the voltage stabilizes, whereas previously it took approximately 5 seconds to stabilize. Another point to note is that there is less change in the load during a load change at 30 seconds.

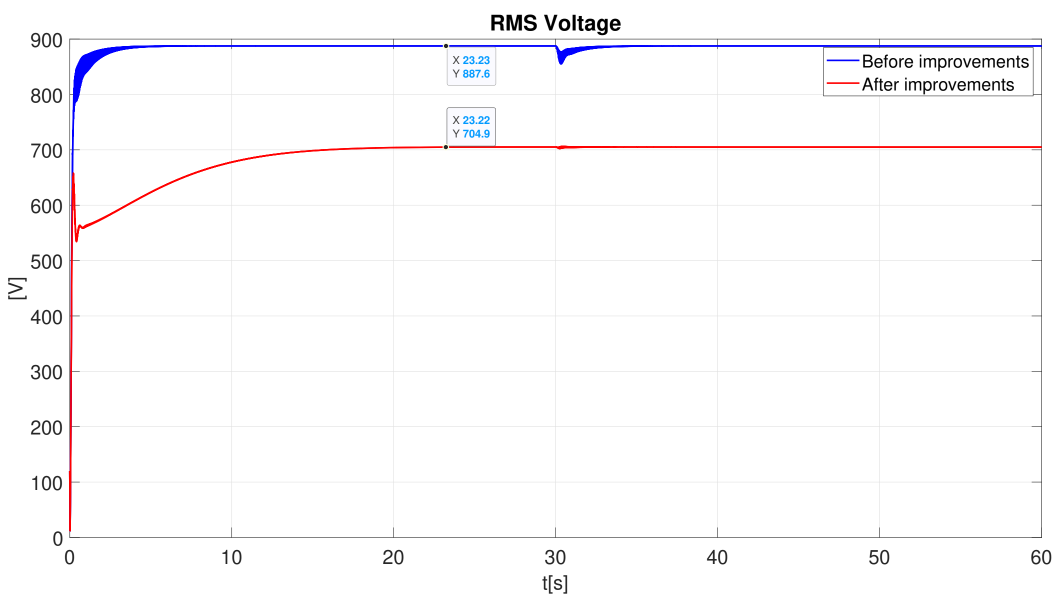

Figure 23: RMS voltage for the analytical model before and after improvements

5.1.2 Normal parallel operation

For the rest of the simulations, the simulation time was decreased from 60 seconds to 30 seconds. In this case, there were two synchronous generators operating in parallel, and both generators were operating at nominal speed and supplying a constant voltage load of 0.4Ω. Figure 24 shows the DC voltage for the analytical and detailed models during this simulation. It can be seen that the voltage value for the analytical model changes a little during the whole simulation. It oscillates from 913V to 965V. This is an acceptable value, considering the voltage should be 952V. The voltage stabilizes after about 15 seconds, which is relatively slow.

It can also be observed that the voltage for the detailed model is very similar to the analytical model. The voltage peak at the beginning is much higher at over 1300V, while it is only over 1100V for the analytical model. The voltage oscillates between 909V and 955V, which is quite similar to the analytical model. There is a slight drop at the beginning for the detailed model, which means it is slower than the analytical model to achieve nominal voltage.

Figure 25 shows the power for the two generators and also the power measured for the DC load. It can be seen that each generator supplies a power load of 1131kW, which when combined is the same as the DC load at 2252kW.

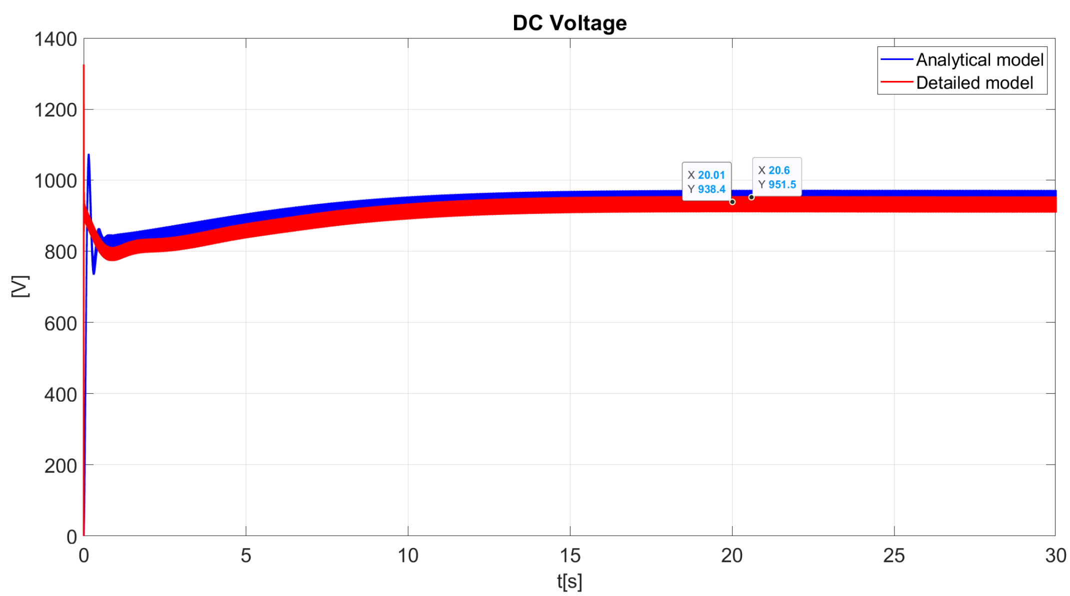

Figure 24: DC voltage for parallel operation for analytical model and detailed model

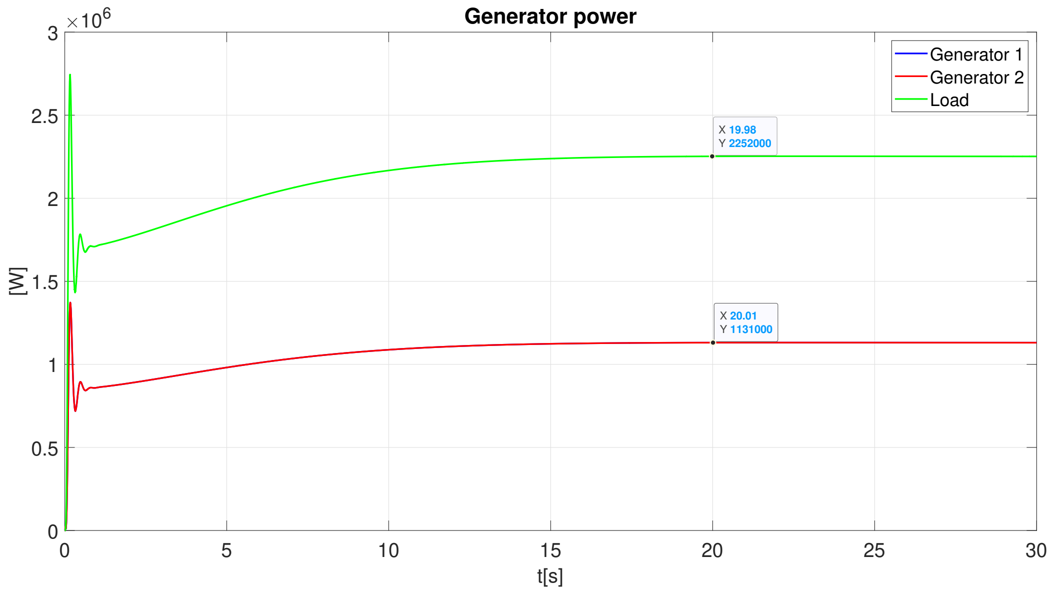

Figure 25: Power for generators and load

5.1.3 Load change

In this case, a change in the load occurs after 20 seconds. Following this, additional resistance with the value 1Ω is added to the system. The DC voltage for simulations with and without droop control can be seen in Figure 26. The power supplied from each generator and also the power to the load is seen in Figures 27 and 28. The DC voltage is quite similar with and without droop, but it should be noted that there is no drop in the voltage when there is no droop. The power loads are also quite similar but are slightly lower with droop control. Both generators have the same droop constant of 0.05.

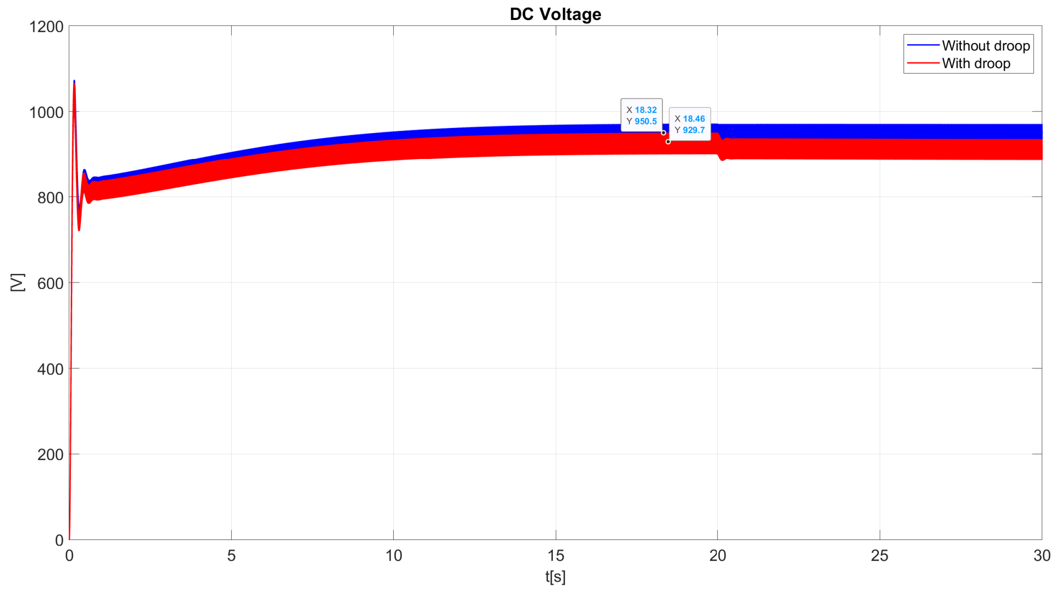

Figure 26: DC voltage for parallel operation with change in load with and without droop control

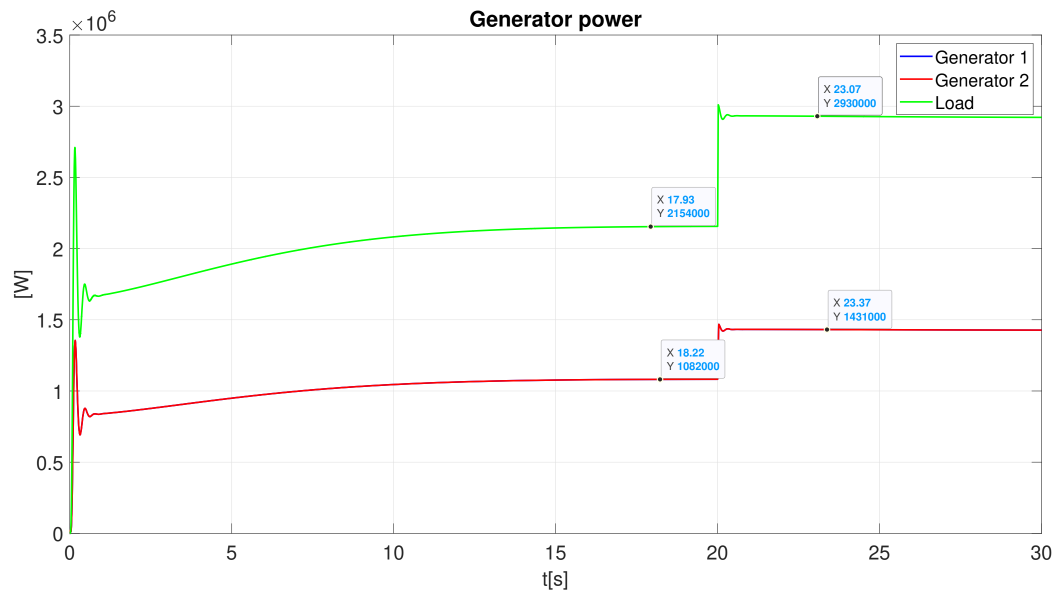

Figure 27: Power supplied from each generator and to the load with droop control

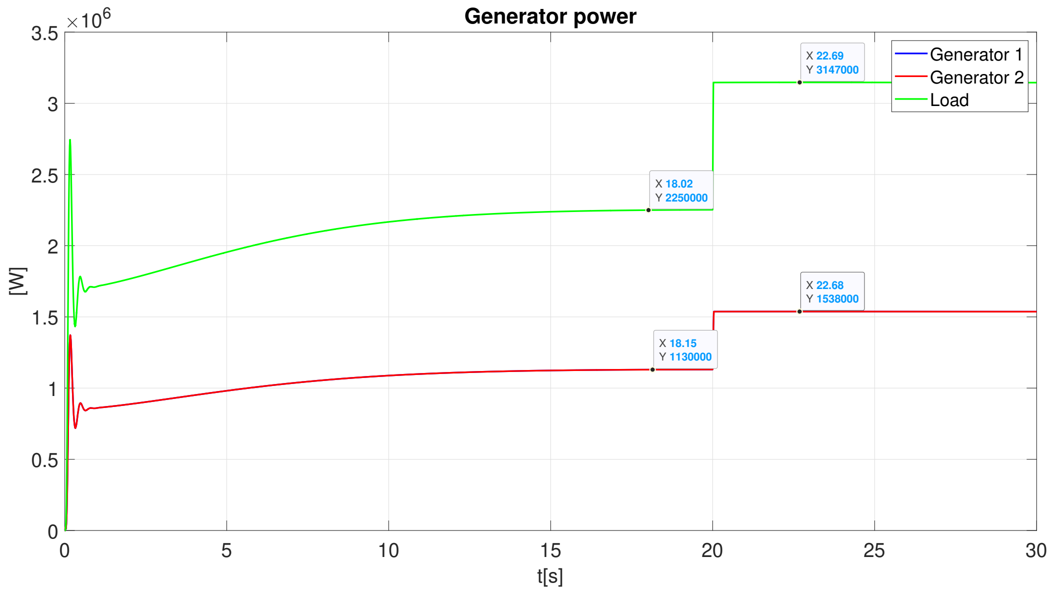

Figure 28: Power supplied from each generator and to the load without droop control

On changing the droop constant for Generator 2 to 0.04, the results change. These results can be seen in Figures 29, 30 and 31. The DC voltage in Figure 29 is at 929.4V, which is close to what it should be. This is also the case after the load change, when the voltage drops to 923.1V. Since there is no variable speed operation for this case, the speed for the generators will be constant at 1000RPM. From the power supply for the generators in Figure 31, it is possible to see the effect of the different droops. Generator 2 has the lowest droop, which means that it will supply most of the power in the load. Figure 31 shows that Generator 2 supplies 2117kW before the load change, which is basically all the load, while Generator 1 supplies 796.7kW. This provides a total of 2913.7kW before the load change. This is approximately 700kW more than the load. Figure 32 illustrates the root mean square (RMS) voltage for each generator and it shows that the voltage for Generator 1 is 5.9V lower than the voltage for Generator 2. This difference shows that the AC voltage is not adjusted with the droop.

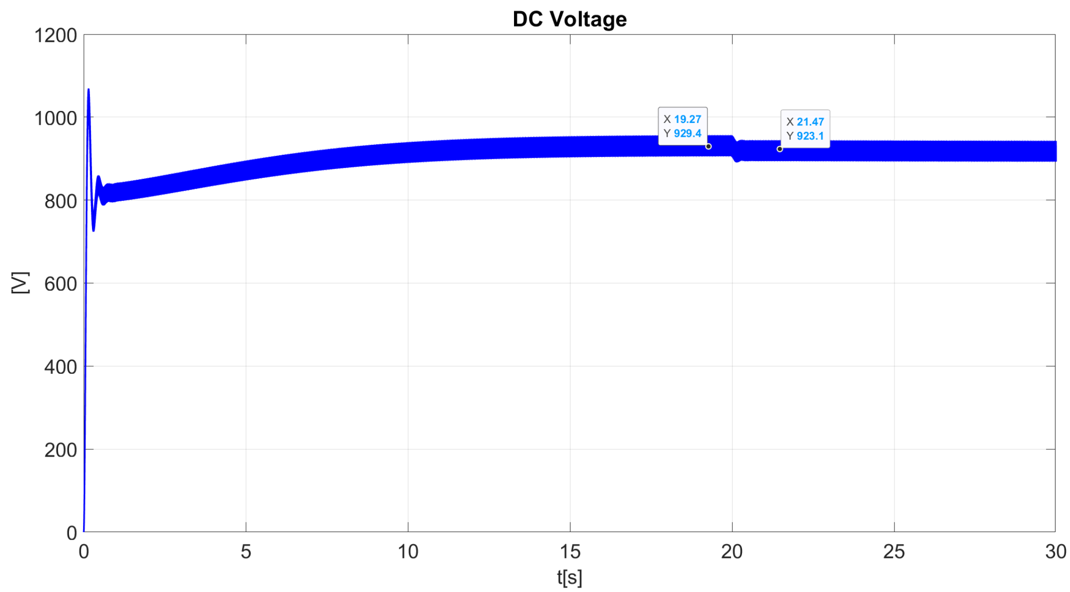

Figure 29: DC voltage for the system with different droops for the generators

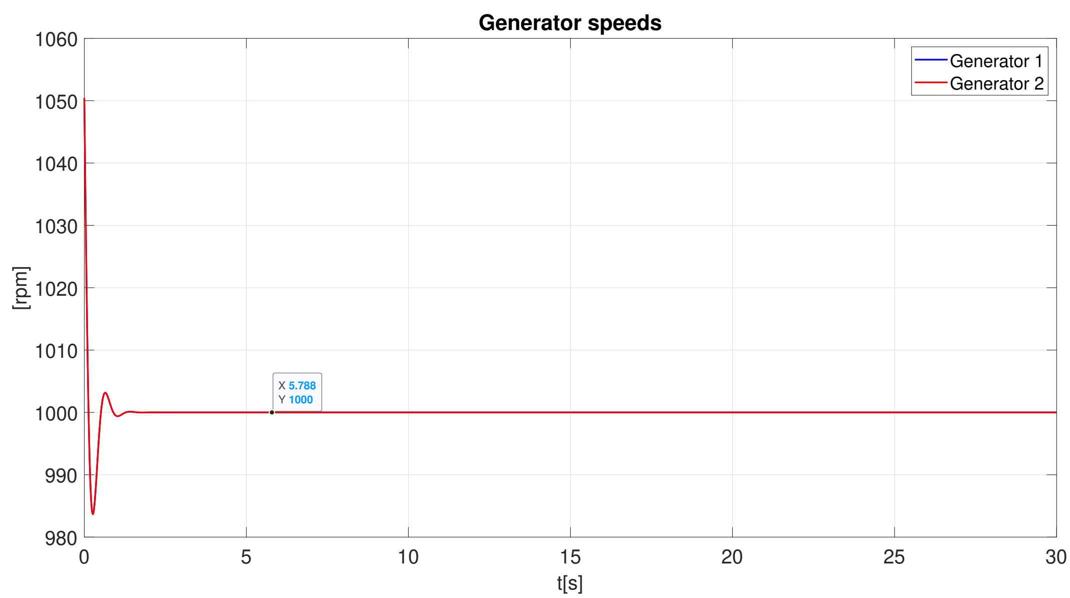

Figure 30: Speed for both generators with different droops for the generators

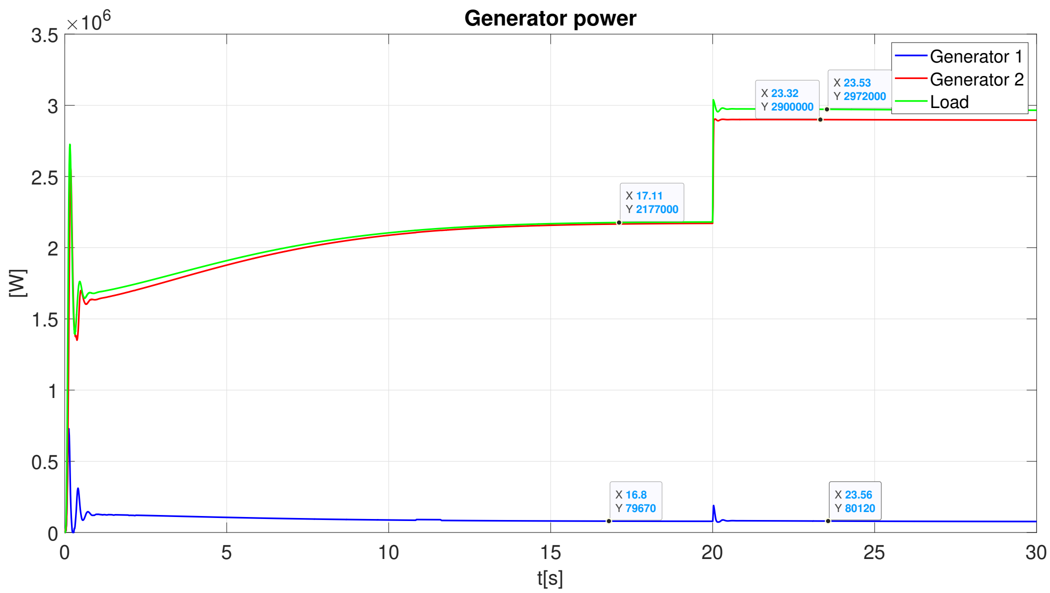

Figure 31: Power supplied from each generator with different droops for the generators

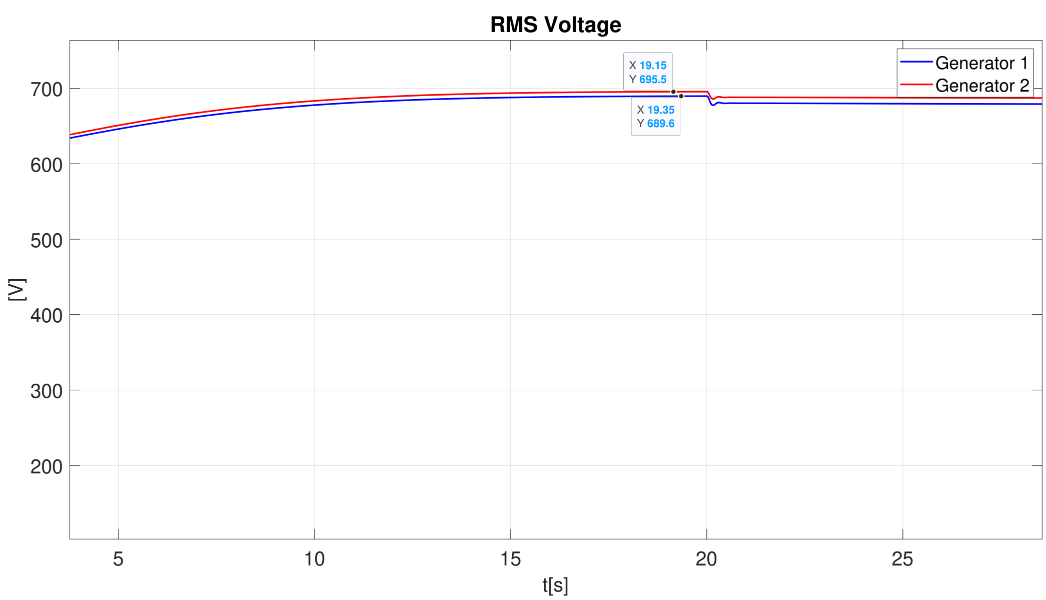

Figure 32: RMS voltage for each generator with different droops for the generators

5.1.4 Variable speed operation with one generator

Different cases for variable speed operation were simulated during this project. Using a load limit curve for the generators allows the different energy consumption for the different speeds to be observed along with how much power can be gained from each cylinder. From the load limit curve, it is possible to see that if 150kW is desired from all the cylinders, there is an energy consumption of 8600kJ/KWH at 1000rpm. If the speed is reduced from 1000rpm to 800rpm, the fuel consumption can also be reduced to 8080kJ/kWh for each of the nine cylinders. This provides a total fuel reduction of $9 \cdot 8080 kJ/kWh = 72720 kJ/kWh$ per generator. The possibility also exists of running one generator at full speed and the other generator at lower speed. The load limit curve for generator is not included in the project due to uncertainties with confidentiality, but an example of such a curve can be seen in Figure 4.

Figure 33 shows how much energy the generator requires to produce a certain amount of power. The red curve shows the energy consumption if the speed is fixed at 1000RPM, which will be the case if there is no variable speed operation. The blue curve shows the energy consumption when the speed of the generator is set to the optimal speed for the power generated. From this curve, it can be seen that with larger loads, there is less effect from the variable speed operation, while it is possible to save considerable fuel by decreasing the speed for smaller loads. At a load of 540kW, there is a difference of 19800kJ/kWh at 1000RPM and 600RPM.

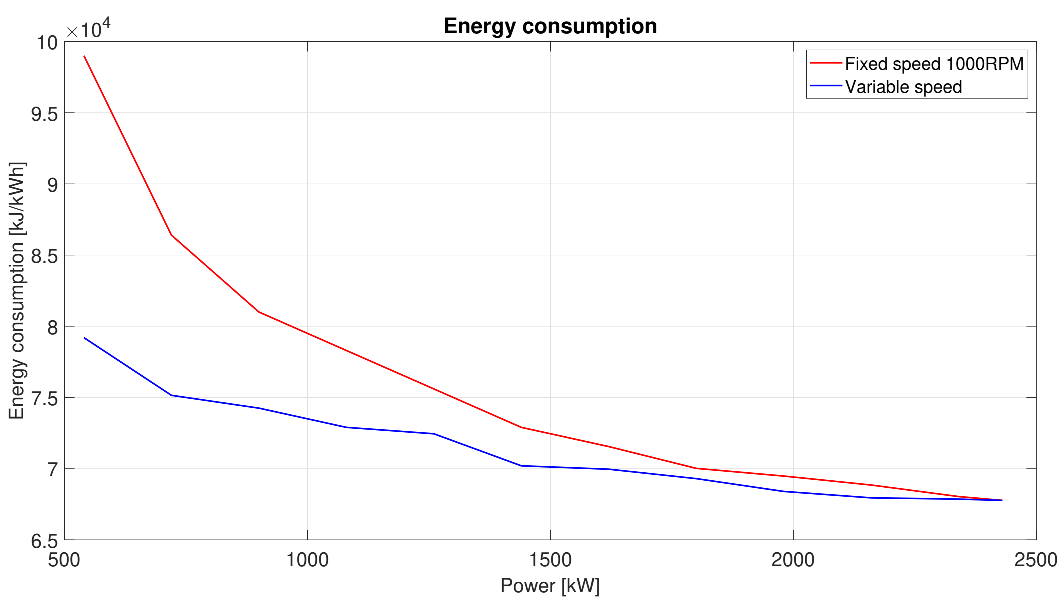

Figure 33: Energy consumption for one generator

A case with variable speed for one generator was tested. In this case, there was a load change, but this load change was smaller than the load change cases tested earlier. A load of 3Ω was added to the system, which produced a total load of 2562kW. The speed of the generator can be seen in Figure 34. Before the load change, the speed is 980.8RPM, and after the load change, the speed changes to 996.6RPM. In Figure 35 it can be observed that the voltage before the load change is 944V and 943.6V after the change. These numbers indicate that there is a minimal change before and after the load change. The power supplied from the generator can be seen in figure 36. The power supplied before the load change is 2243kW and 2532kW after the load change.

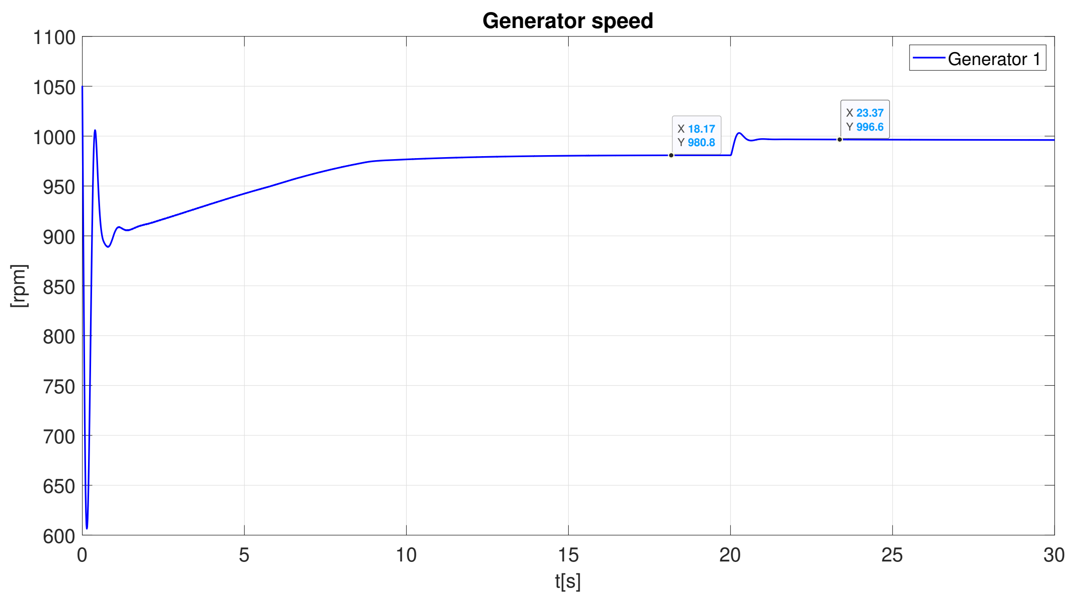

Figure 34: Engine speed for one generator during a load change

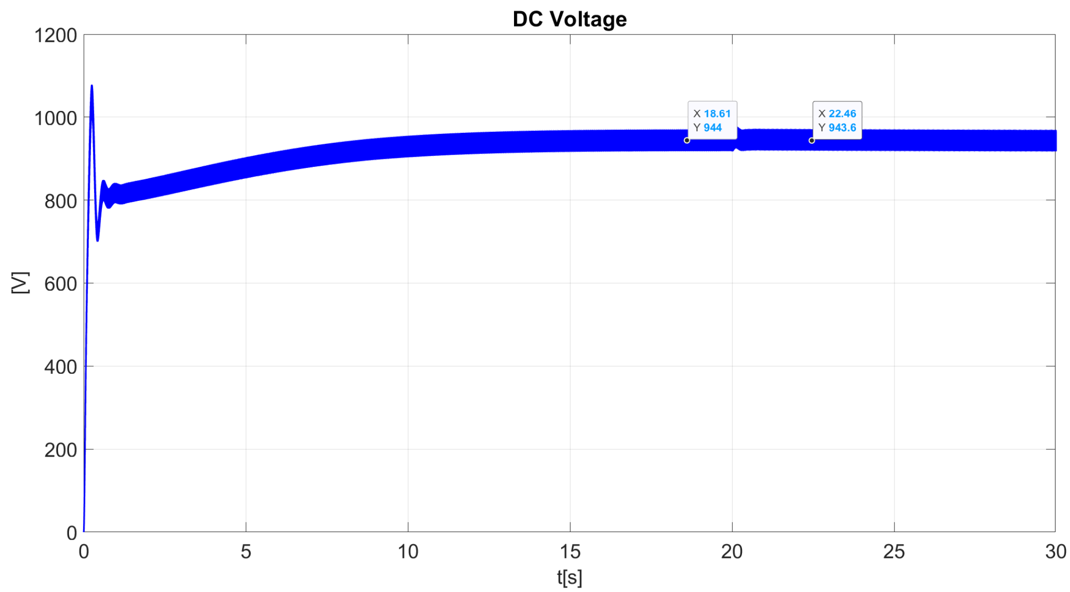

Figure 35: DC voltage for one generator during a load change

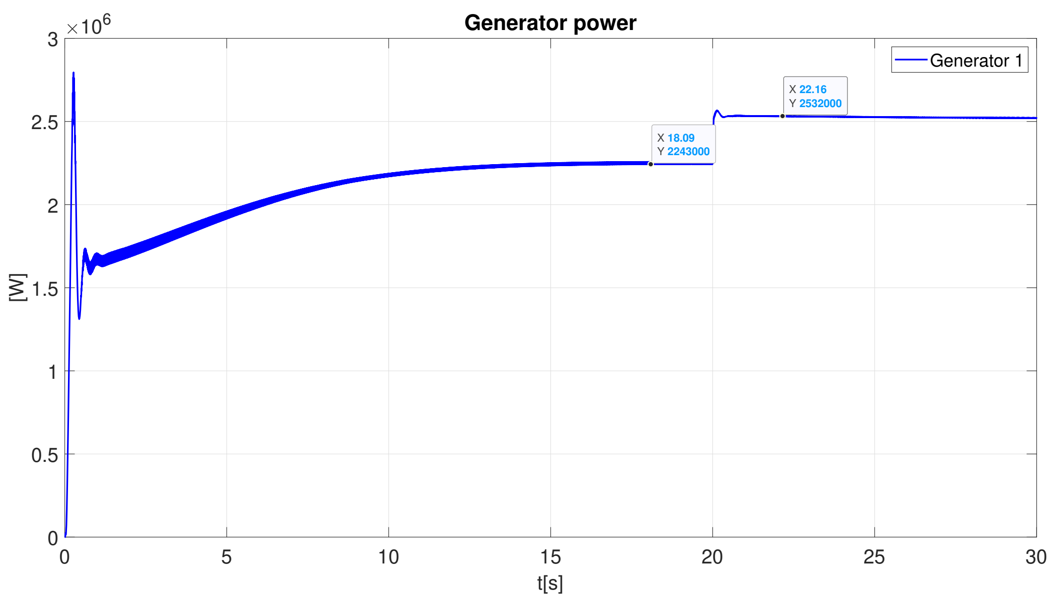

Figure 36: Power for one generator during a load change

5.1.5 Variable speed operation in parallel

First, the variable speed operation was tested without droop control. In this case, there is a load change at 20 seconds when the load goes from 2261kW to 3118kW. Both generators have variable speed operation. There was no droop control for the voltage for this case, which means that both generators should supply the same amount. Figure 37 shows how the DC voltage behaved during this variable-speed operation. Before the load change, the DC voltage was 1069V, and after the load change, it increased to 1082V. The speeds for both generators are shown in Figure 38. Both generators are at a speed of 921.8RPM before the load change and 994.1RPM after the change. Figure 39 shows the power for both generators. They supplied the same amount of power and each supplied 1779kW before and 2486kW after the load change. This is much higher than the load.

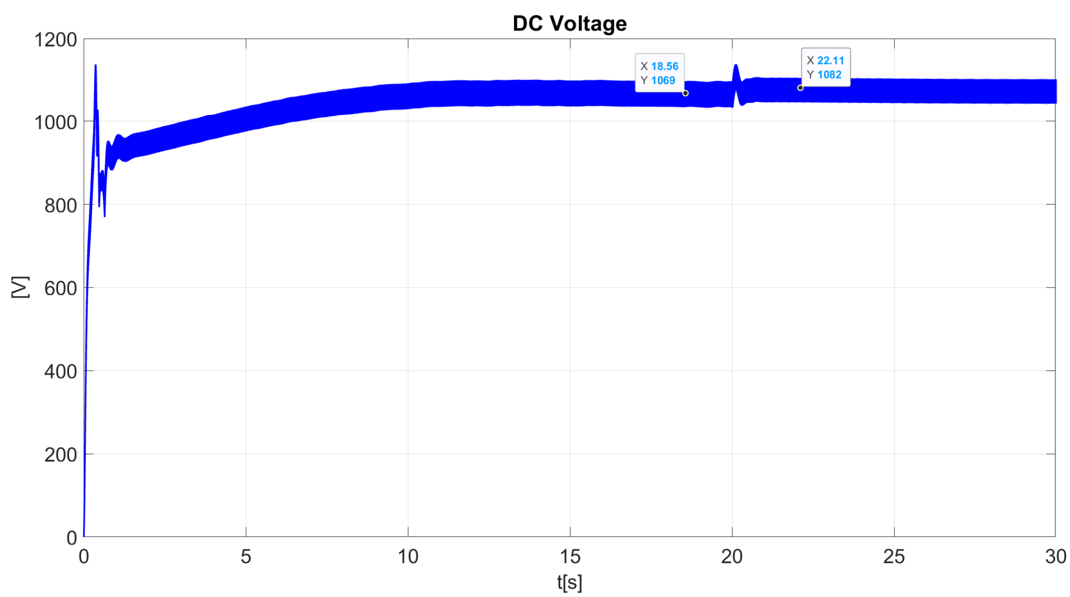

Figure 37: DC voltage for variable speed operation of parallel generators

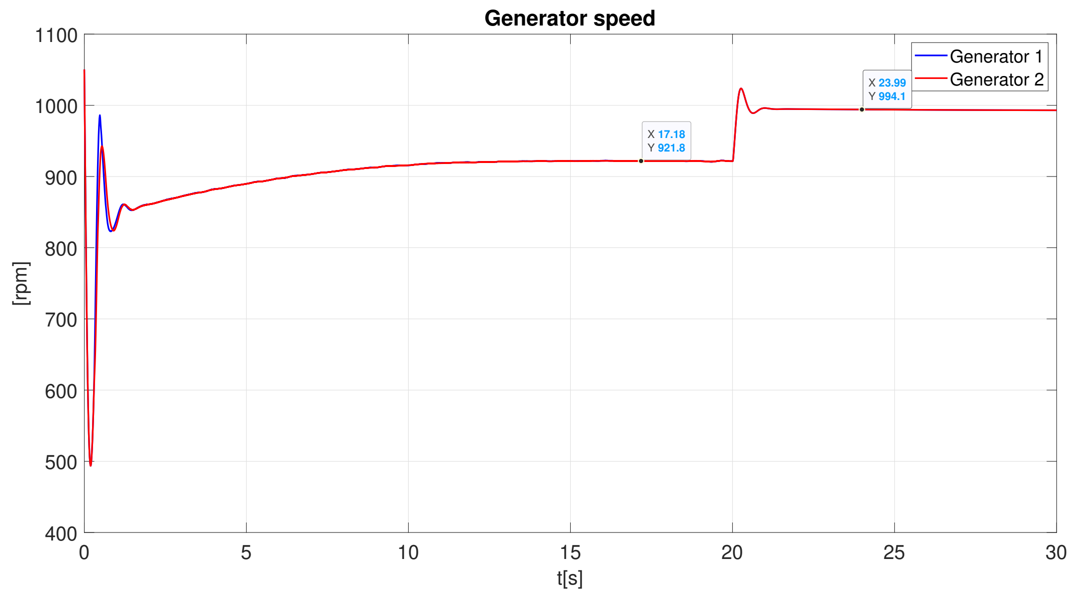

Figure 38: Generator speed for both generators during variable speed operation

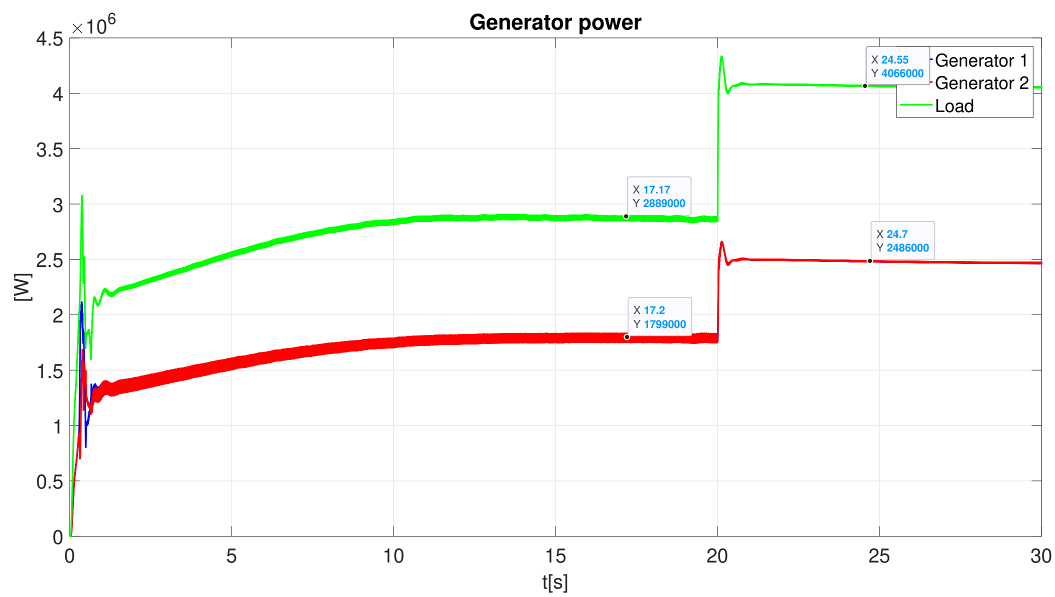

Figure 39: Power supplied from each generator

A new case was then tested. The premise was very similar to the previous case, but the reference voltage for the excitation system was switched with droop control. Figures 40, 41 and 42 show what the results were when both generators had the same droop. Both generators had droop constants of $\delta = 0.05$, which meant that both generators had a droop of 5%. Figure 40 shows that the DC voltage for this case was 1041V before the load change and 1029V after the load change. The speed in Figure 41 shows that the speed increase from 907.1RPM to 980.9RPM after the load change. Both generators supplied 1667kW before the load change and 2249kW after the change. This can be seen in Figure 42. The RMS voltages for the two generators are presented in Figure 43, in which it can be seen that the voltage is 680.8V.

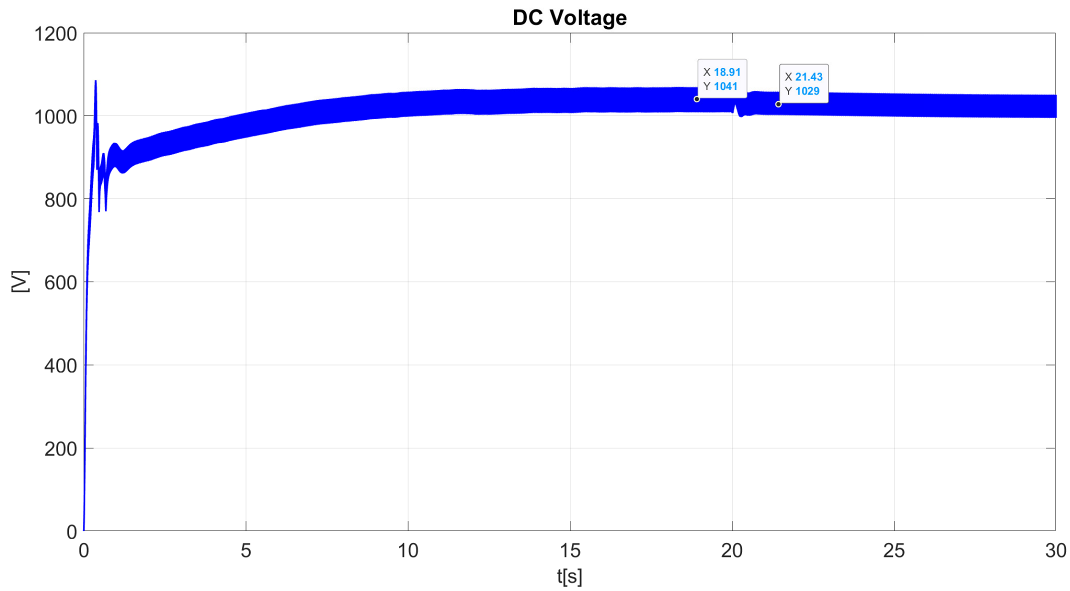

Figure 40: DC voltage with same droop for both generators

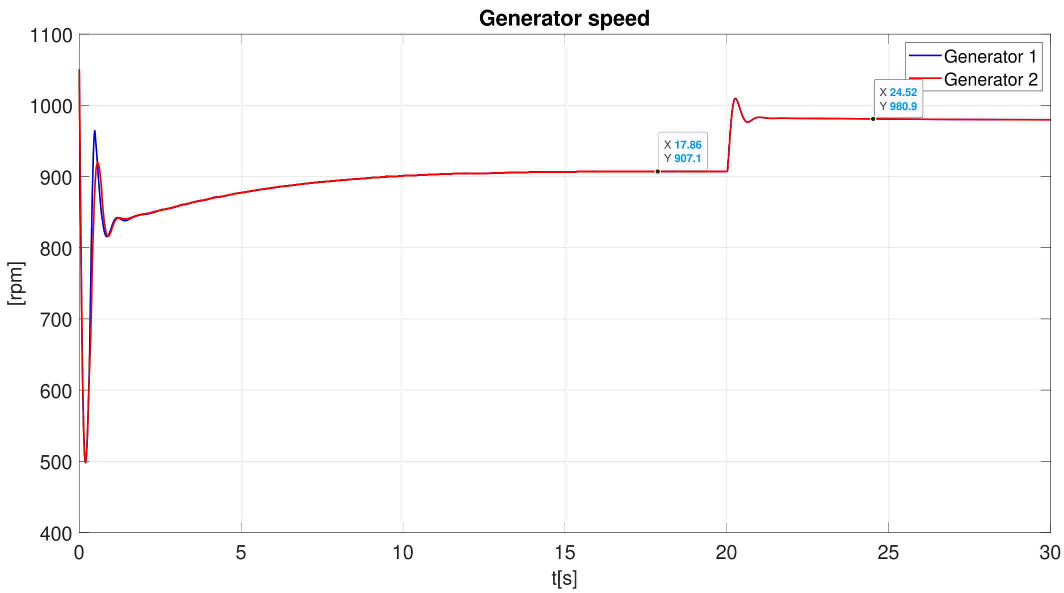

Figure 41: Speed for each generator with the same droop

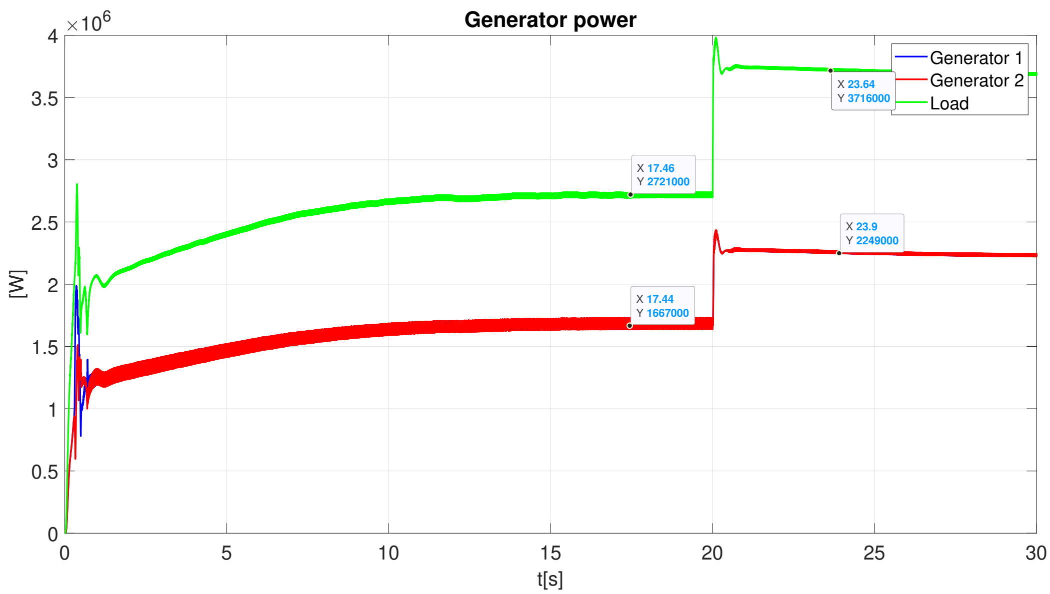

Figure 42: Power supplied from each generator with the same droop

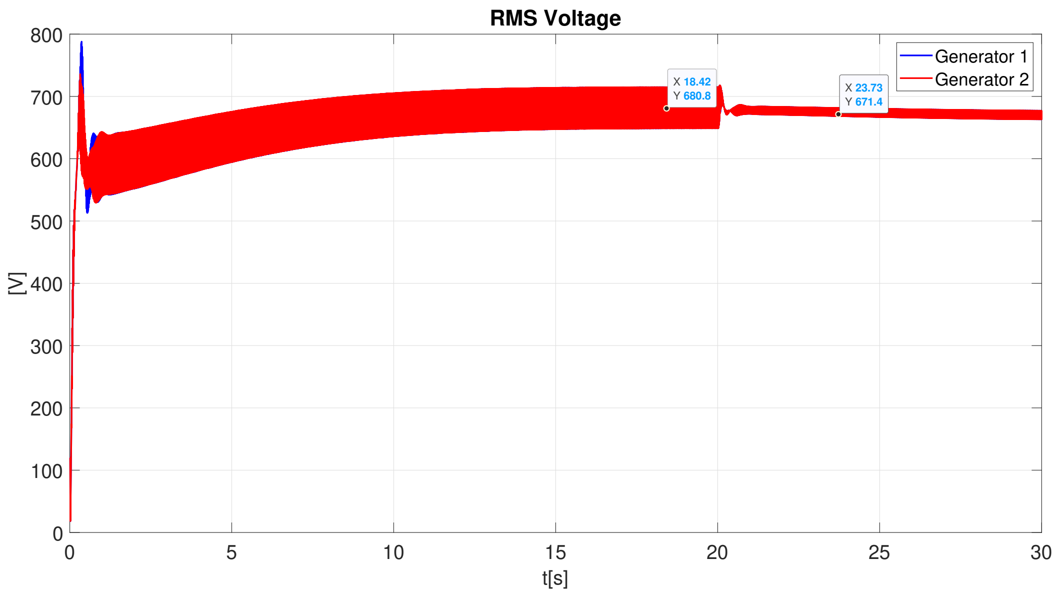

Figure 43: RMS voltage for each generator with same droop for both generators

The droop for Generator 2 was changed to $\delta = 0.04$ to observe how the two generators behaved with different droops, which meant that this generator should have supplied more than Generator 1. These results can be seen in Figure 44, 45 and 46. In this case, the results were much more unstable, but they were around the same values as when they had the same droop. It can be seen from the two plots for power and speed that Generator 2 has slightly higher values than Generator 1, but this is difficult to distinguish due to the instability.

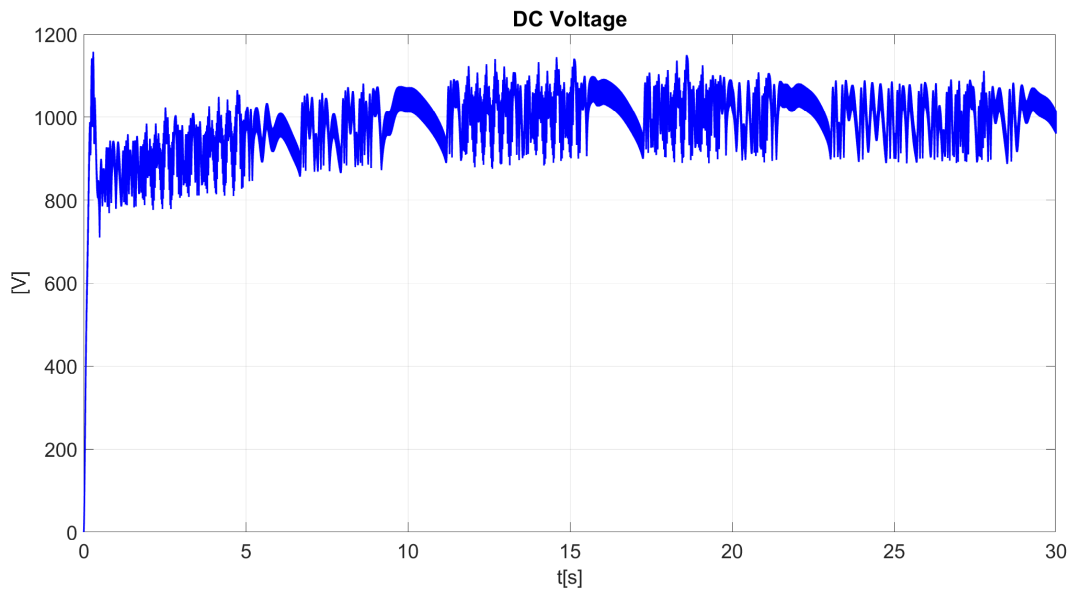

Figure 44: DC voltage with with 4% droop for generator 2 and 5% for generator 1.

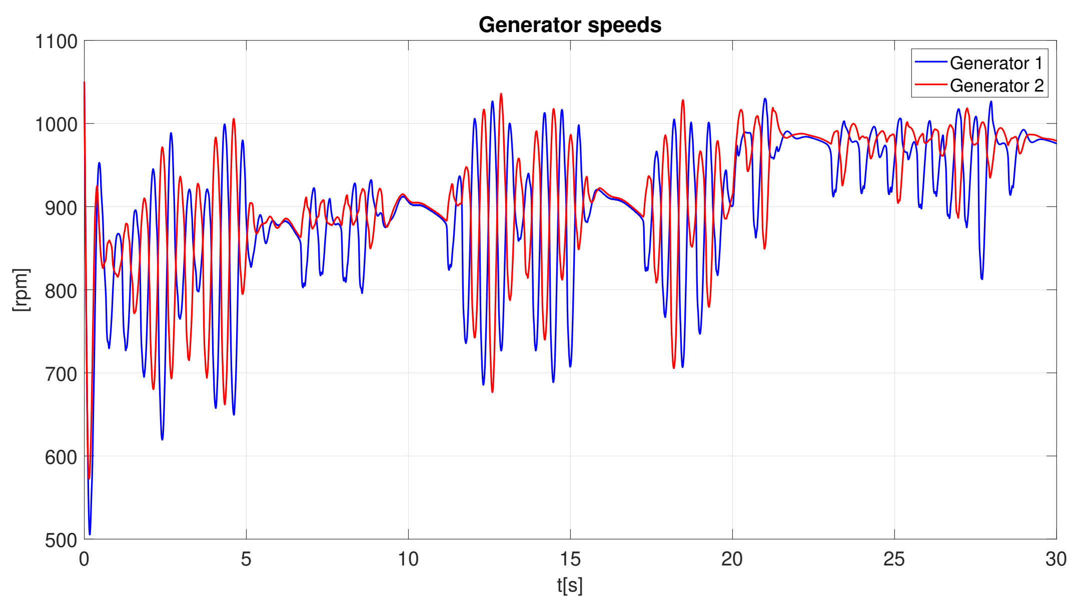

Figure 45: Speed for each generator with 4% droop for generator 2 and 5% for generator 1.

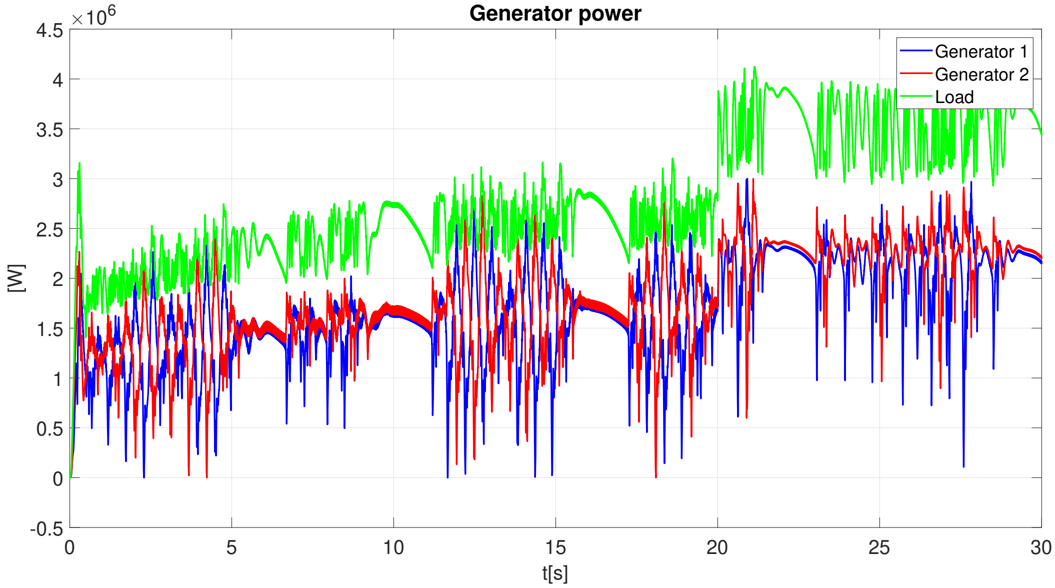

Figure 46: Power supplied from each generator with 4% droop for generator 2 and 5% for generator 1.

The droop constant of Generator 1 was changed to 0.1 or 10%, while Generator 2 had a droop of 0.05 or 5%. This alteration was undertaken to see whether changing the droop constant would affect the system. The power supplied from each generator is shown in Figure 47 where it is possible to see that Generator 2 supplied more power than Generator 1.

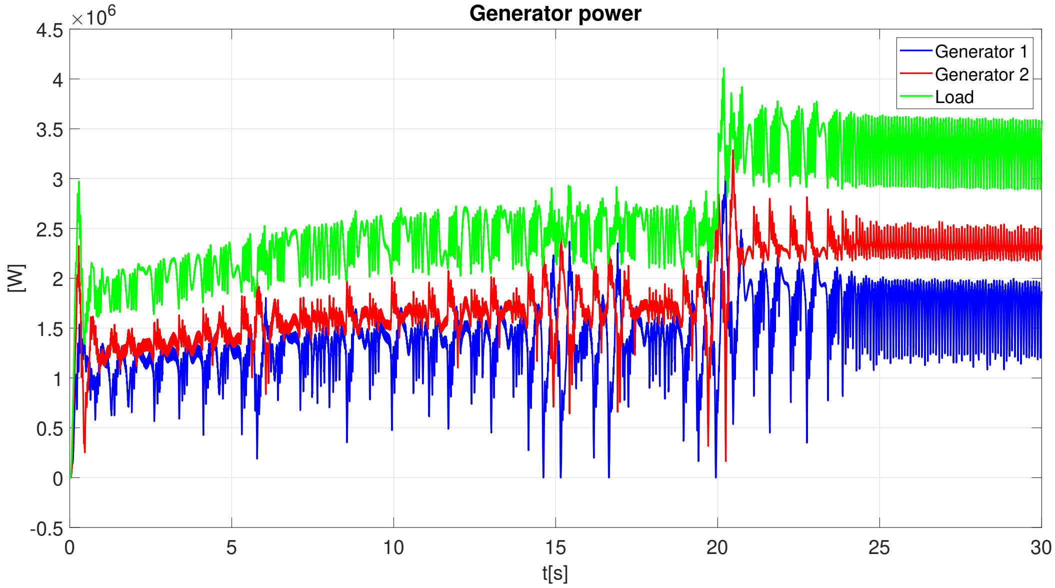

Figure 47: Power supplied from each generator with 5% droop for generator 2 and 10% for generator 1.

The instabilities that occur during variable speed operations with different droops can be caused by the two generators operating at different speeds, making the results messier. Therefore, tests were performed using the same variable speed for both generators. This meant that either the power from Generator 1 or 2 decides the speed at which both generators operated. This was first tested with Generator 2 setting the speed for both generators. The results can be seen in Figure 48, 49 and 50. In this case, Generator 2 supplied basically all the power, which is 2152kW. Since Generator 2 is the one that decides the speed of both generators, the speed was 975.3RPM before the load change, which is set by the lookup table considering the power supplied from Generator 2. The system also appeared more stable than previously.

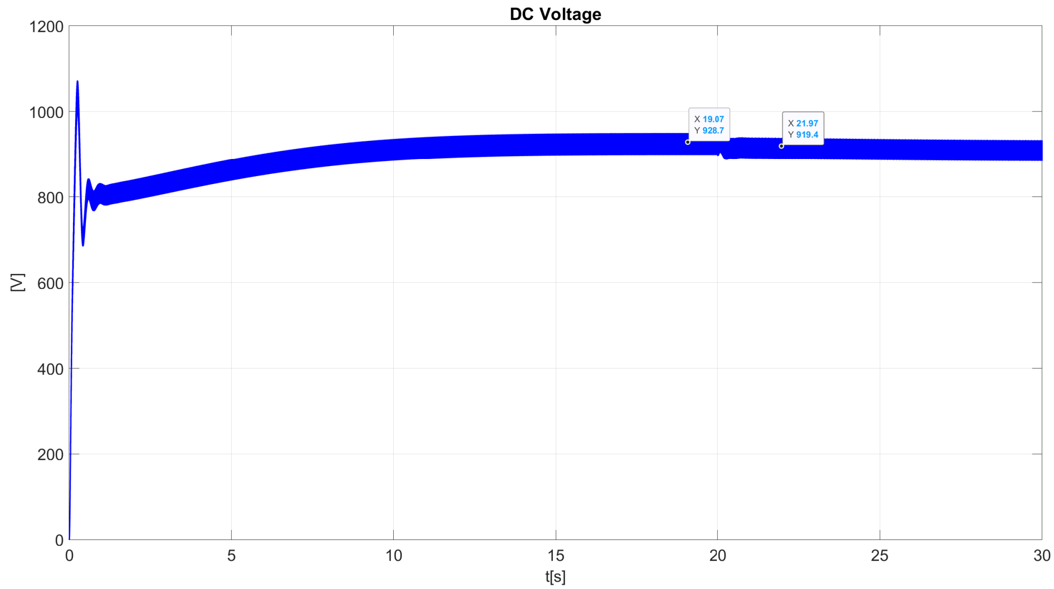

Figure 48: DC voltage with variable speed controlled by generator 2 with 5% droop for generator 2 and 10% for generator 1.

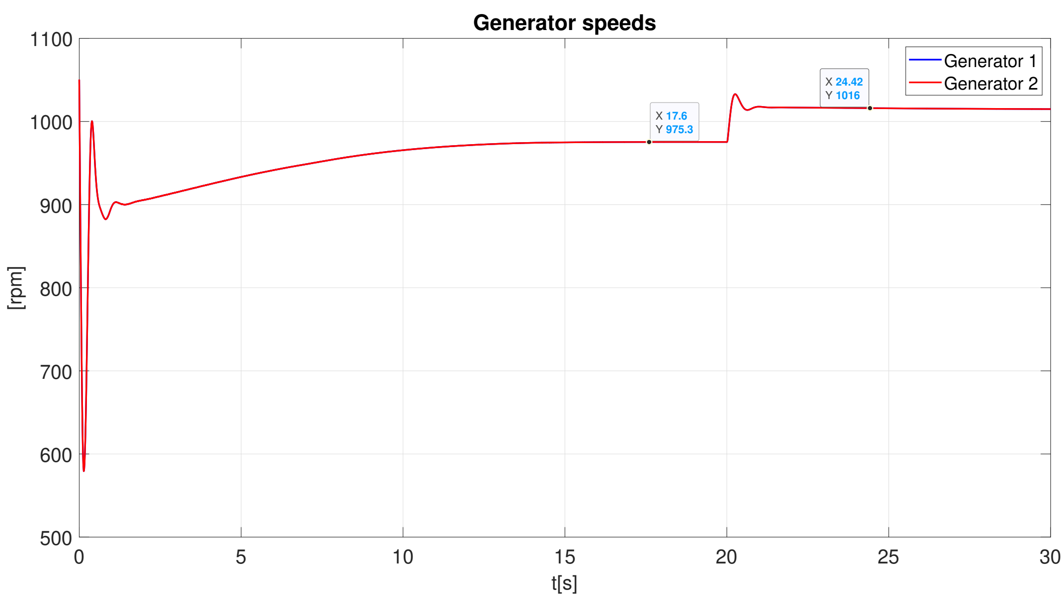

Figure 49: Speed for both generators with variable speed controlled by generator 2 with 5% droop for generator 2 and 10% for generator 1.

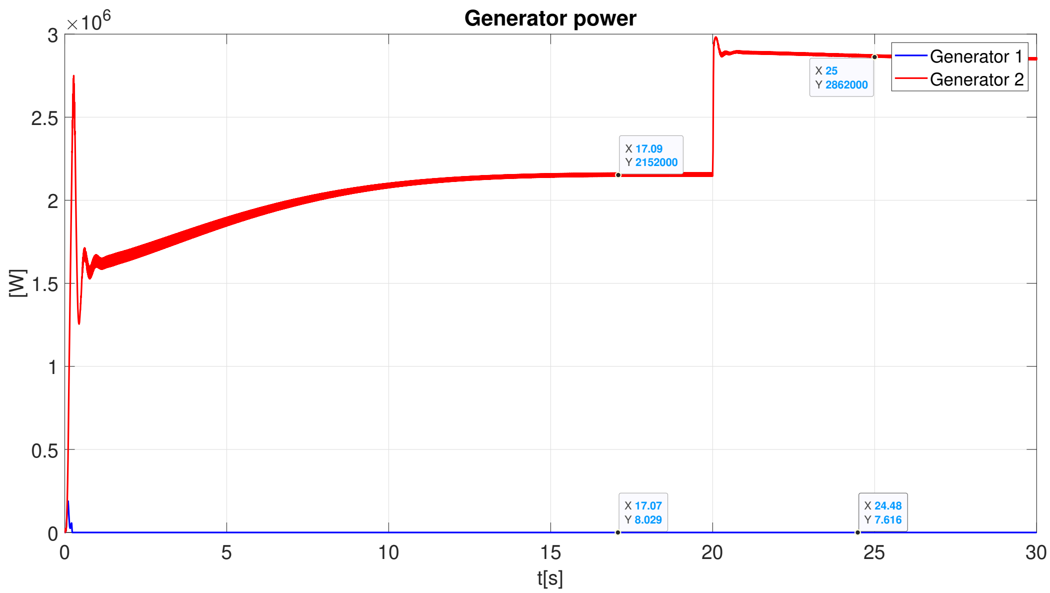

Figure 50: Power supplied from both generators with variable speed controlled by generator 2 with 5% droop for generator 2 and 10% for generator 1.

The same test was also performed with Generator 1 controlling the speed for both generators. The results can be seen in Figure 51, 52 and 53. The DC voltage was 922.4V before the load change. Both generators operated at a speed of 500RPM. Generator 1 supplied 2057kW, while generator 2 supplied essentially nothing.

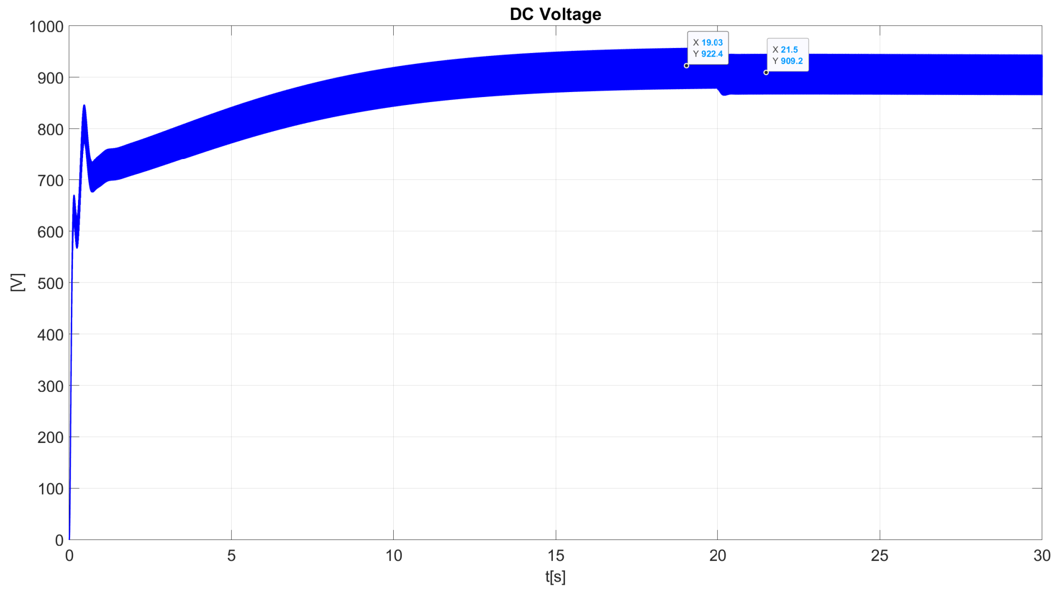

Figure 51: DC voltage with variable speed controlled by generator 1 with 5% droop for generator 2 and 10% for generator 1.

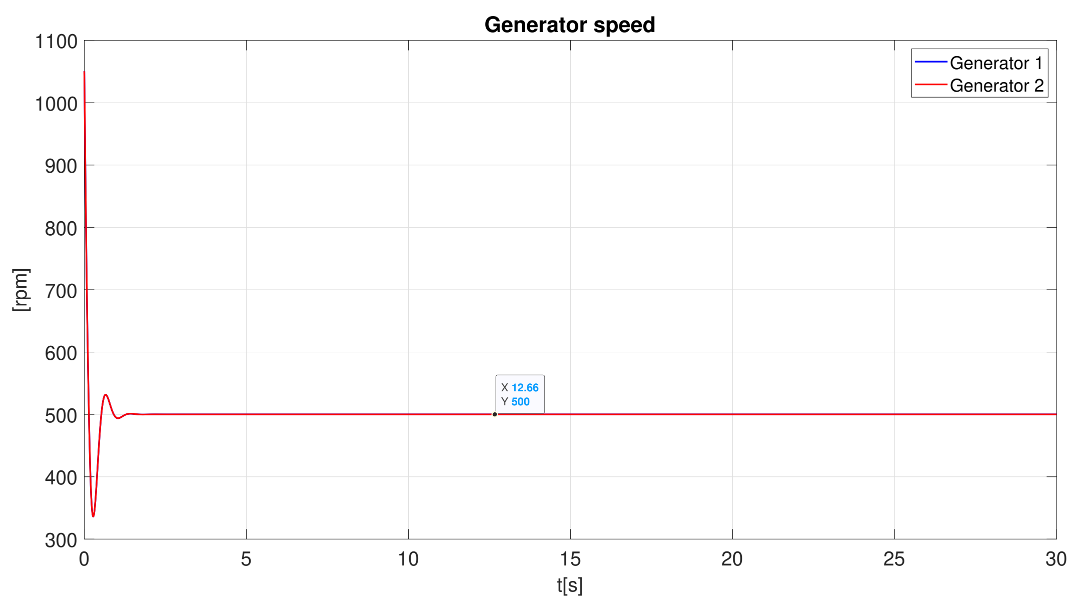

Figure 52: Speed for both generators with variable speed controlled by generator 1 with 5% droop for generator 2 and 10% for generator 1.

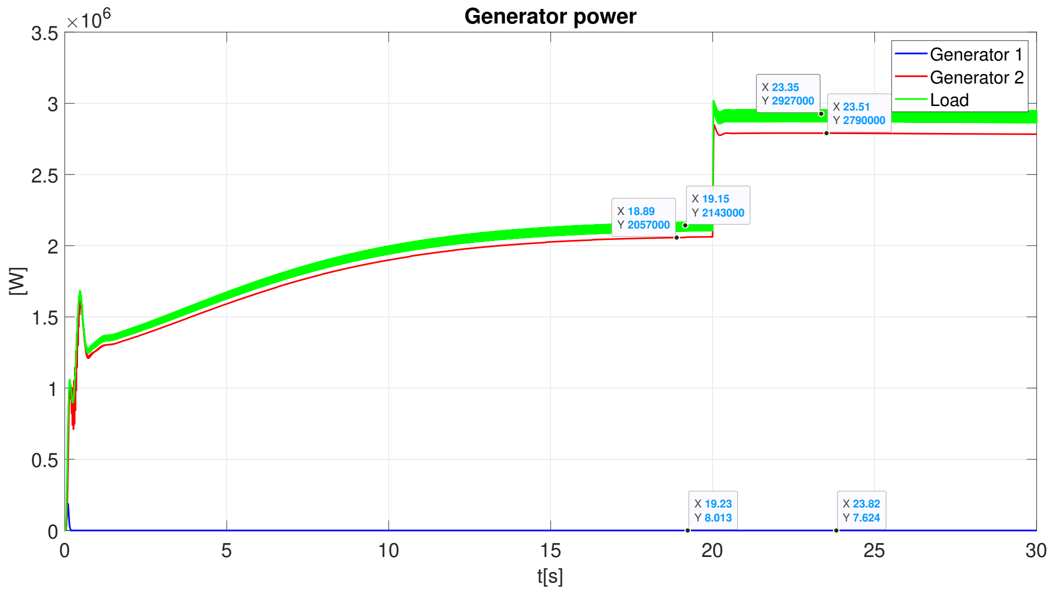

Figure 53: Power supplied from both generators with variable speed controlled by generator 1 with 5% droop for generator 2 and 10% for generator 1.

5.1.6 Switching governor

The original governor from Figure 11 was switched with the governor from Figure 12 to ascertain whether the instabilities were due to the governor. Since there was no speed droop control in the previous cases, the droop for the governor was set at 5% for both generators to prevent it from affecting the droop control used for the excitation system. There may still be some offset to the speed due to the droop for the governor. This occurs when Generator 1 has a voltage droop of 10%, and Generator 2 has a droop of 5%. Both generators also have their own variable speed controllers. The results are shown in Figure 54, 55 and 56.

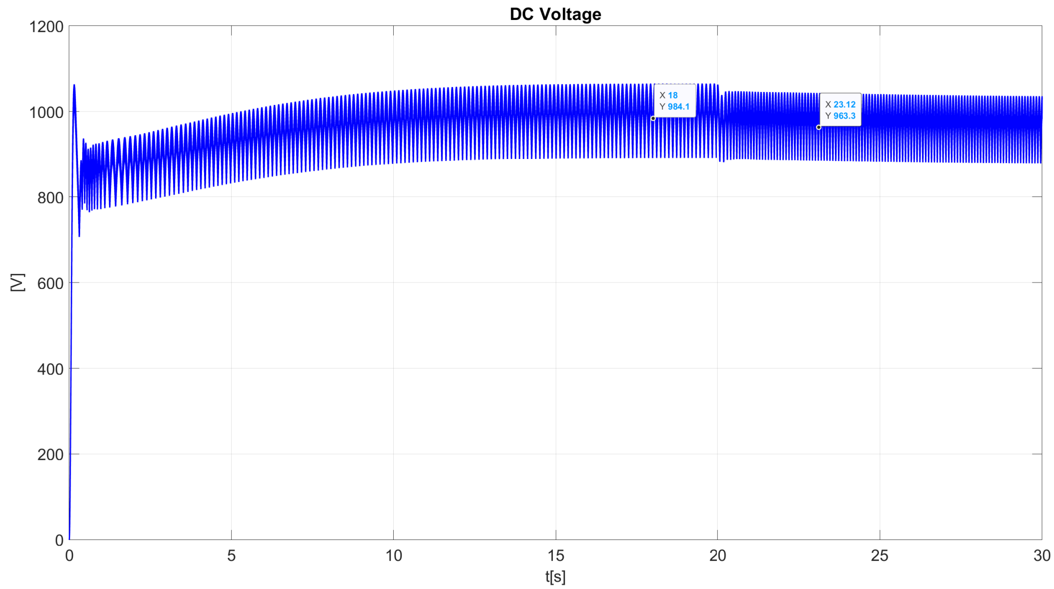

Figure 54: DC voltage with variable speed controlled by generator 2 with 5% droop for generator 1 and 10% for generator 1. Governor is switched out with other model.

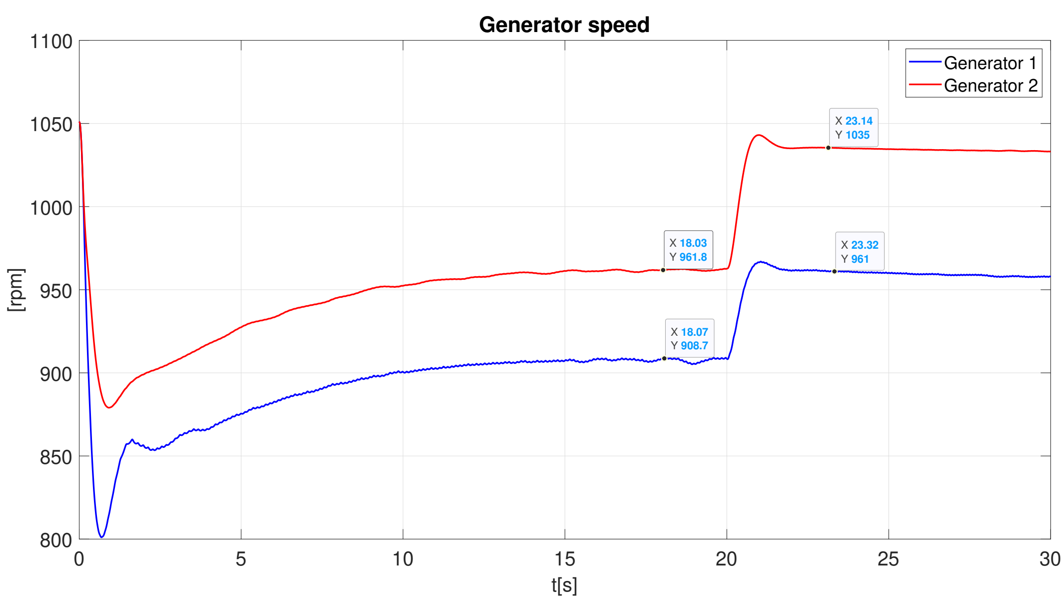

Figure 55: Speed for both generators with variable speed controlled by generator 2 with 5% droop for generator 1 and 10% for generator 1. Governor is switched out with other model.

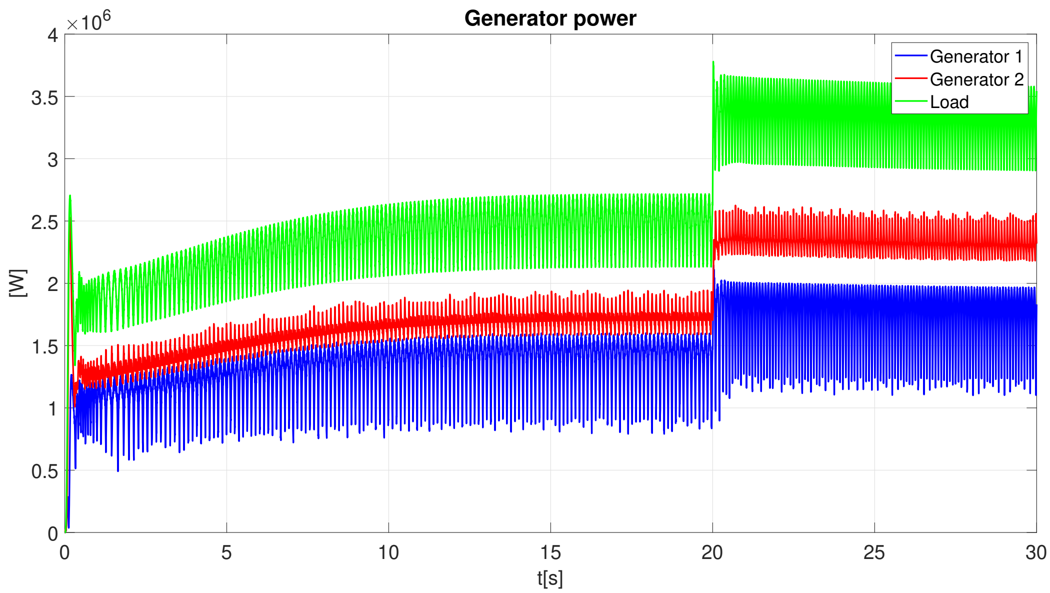

Figure 56: Power supplied from both generators with variable speed controlled by generator 1 with 5% droop for generator 2 and 10% for generator 1. Governor is switched out with other model.

5.2 Linear model

The linear model includes the governor, excitation system, and generator. The eigenvalues can be seen in Figure 57. There are a total of eight eigenvalues. Four of the eigenvalues are on the left-hand side of the y-axis and three are on the right-hand side. The last eigenvalue is in origin. There are six eigenvalues that do not have an imaginary part.

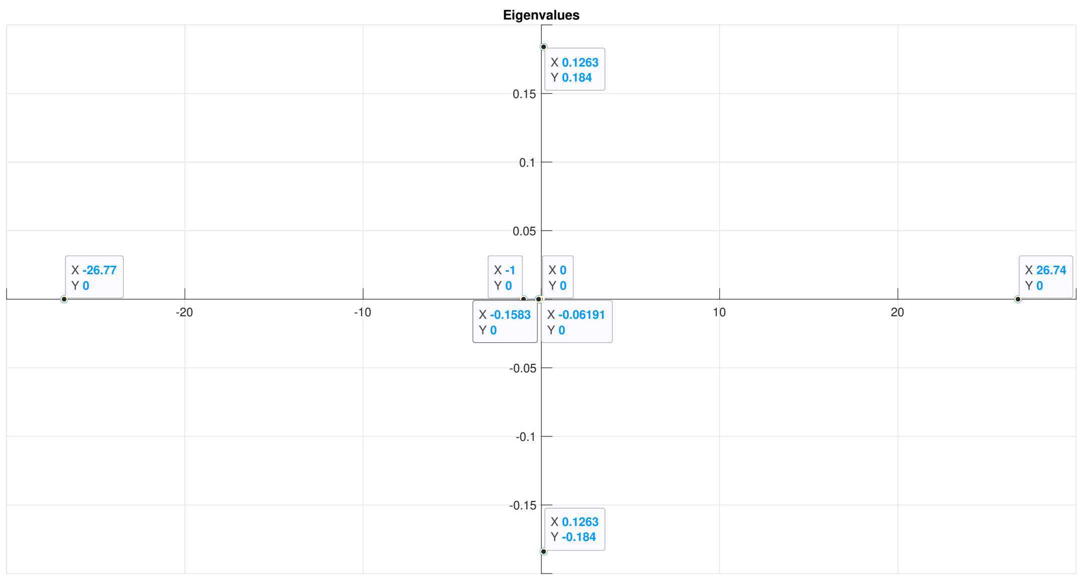

Figure 57: Eigenvalues for the system

6 Discussion

6.1 Improvements for the original model

A few issues with the analytical model from the specialization project needed to be fixed before further advancements with the project could made. These improvements were made before beginning to examine operations in the DC grid and parallel operations. When the analytical model for the synchronous generator gives the wrong values, there is a possibility that the other modeling will be based on these values and therefore be wrong.

One of the issues that needed to be fixed was the dq0-transformation that is carried out on the voltage before it is used in the excitation system. The original dq0-transformation performed with function blocks in Simulink gave a value that always became 1 when calculating the terminal voltage. This fed the value 1 into the excitation system, which tells the excitation system that this is the desired voltage and therefore the system does not change it. This means that even though the voltage is not the desired voltage, the excitation system believes that it is correct.

Another change required for the model was that the base value for the voltage was not correct. The value used was 705V when it should be the peak value $\sqrt{2} \cdot 705V$. There were also some places where per unit values were used when they should not have been used.

6.2 Normal parallel operation

During the operation for the parallel generators, it was observed that the DC voltage for the analytical model and the detailed model were quite similar. They remained close to 950V, which corresponds well with the fact that with a simple diode rectifier, the DC voltage should be $705V * 1.35 = 951.75V$. This can be seen in Figure 24. There appears to be only 13.1V differentiating the two models. From these result it should mean that the analytical model gives the correct result since it matches a model with finished blocks. Another point to note is that if there is an issue with both the models, it should be with the excitation system or the loads since these are the only components that are the same for both models. The power supplied from the analytical model is seen in Figure 24, in which each generator supplies 1131kW. This figure shows that the generator supplies the proper values, and the total amount supplied from both generators is equal to the load.

6.3 Load change

From the case in which an additional load was added, it can be seen that when the system does not have droop control, there will be no change to either the DC voltage or the AC voltage. This is not realistic because there should be some change to the voltage, considering the added load is half of the original load. There will also be some losses for the diode rectifier. When the excitation system has droop control, there is a voltage drop. This drop is because, in a DC system, the load sharing and voltage regulation are made in the excitation system, and with the droop control, the voltage is drooped to manage the load change.

When testing with different droop constants for each generator, there was a large change between the power for each generator. Generator 2 supplied almost all the load while Generator 1 supplied only 37.6% of the amount Generator 2 supplied. Adding the two power measurments together, the power supplied was larger than the load desired. However, even though the two generators supply too much power, the DC voltage is still close to the desired value. It can be seen that there is a minimal change in the voltage, which means that it can be stated that $\Delta V = 0.03pu$ and using Equation 2 it is possible to calculate how much each generator should produce. Generator 1 with $\delta = 0.05$ should produce $\frac{0.03}{0.05} = 0.6pu = 1553.4kW$ and Generator 2 with $\delta = 0.04$ should produce $\frac{0.03}{0.04} = 0.75pu = 1941.75kW$. However, as can be seen from the power actually supplied by the generators, this is not the case. Generator 1 supplies a little over half of the calculated value, while Generator 2 supplies more than the calculated value. This discrepancy indicates that there are some unknown issues with the droop controller for the system.

6.4 Variable speed operation for one generator

For variable speed operation with one generator, it can be observed that the DC voltage is quite similar to the other cases without speed variation. This similarity means that the system operates properly even though the speed changes depending on the power. The load change is smaller in this case than the other since it is only one generator, and the previous load change would be over the capacity of one generator. Figure 34 shows that the speed was originally at 980.8RPM, which is for a load of 2261.1kW. This is a load of 0.87pu, which means that from Table 1, the speed should be a little over 975RPM, which corresponds well with the result. After the load change, the load was 2562kW or 0.99pu, which means that it should be immediately below 1000RPM according to Table 1. This also corresponds well with the result of 996.6RPM after the load change.

6.5 Variable speed operation for two generators

6.5.1 Without droop control

In this case, both generators supply the same amount of power, which means that both generators should have the same speed. In Figure 38 it can be observed that both generators operate at almost precisely the same speed both before and after the load change. One point to note is that Generator 1 has a slightly higher speed in the first few seconds before it settles and behaves similarly to the variable speed case using one generator. There is a difference of approximately 130V between the cases with one and two generators. Considering that, theoretically, the DC voltage should be 970V since the DC reference voltage was set to 1.02 in Figure 14, the variable speed case with two generators is a little further from that with a single generator.

Comparing the speed of Generator 1 before the load change in both single generator operation and parallel operation, it can be seen that the speed is 59RPM slower. This is because the generator supplies half the amount of power in the parallel operation as it does in the single generator operation.

The powers for the generators are higher than they should be. Before the load change, the load is 2261kW, but each generator supplies 1799kW of power, which gives a total power amount of 3598kW, which is much higher than the load. This also occurs after the load change, when the generators supply a total of 4972kW when the load is only 3118kW. This is likely to be the reason that the DC voltage is also too high. The speed is also higher than expected, which is the result of the generators supplying more power than expected.

6.5.2 With droop control

For the first case with droop control, in which both generators have the same droop constant, the DC voltage was approximately 33V lower than for the case without droop control. This is still a little higher than it should be. Both the speed and power were also too high, but the speed is higher due to the variable speed operation, which sets the speed reference according to the power. The speed should not exceed 1000RPM, which is the maximum speed. Since the power is too high, the speed will also be too high. Before the load change, one of the generators supplied 79% of the load, and considering that both generators supply the same amount, they supply far too much power. Examining at the power supplied and the DC voltage, it can be noted that there is minor instability at the start of the simulation. Examining the speeds during this instability, the two speeds are not the same at this time. The peak of Generator 1 was higher than for Generator 2. This may be the reason for the instability of the power and DC voltage.

On changing the droop constant for Generator 2 to 0.04, instability occurs in the system. Even though there is an instability that makes all the values change considerably, some similarities make it appear that the average values for the results with different droops will be quite similar to the case with the same droop constant for both generators. Even though the droop constant for each generator is no longer the same, the values are still quite similar. It appears that the power and speed for Generator 2 are slightly higher, which makes sense considering that it has the smallest droop constant, which means that it should supply the most. The change would be larger if the difference in droop was larger but comparable with the results where the droops are different. However, with no variable speed, there are significantly larger differences between the two generators.

Comparing this result with the droop control results without variable speed operation, there is a noticeably larger difference in each generator's power. Even though there is a slight difference of 0.01 between the droop of the two generators, it is almost impossible to notice the difference between the power of the two generators during variable speed operation. However, in the case without variable speed operation, Generator 2 supplies almost four times as much power as Generator 1. This is likely to mean that there is a problem with operating the variable speed together with the droop control. This can also be seen from the results where they are working alone and provide results that make sense.

One point to note is that for the cases with generators in parallel and with variable speed, the voltage is often a little higher than for the other cases. It is, on average, about 100V higher than in the other cases. The power supplied is also higher for many cases with variable speed operation. Examining the RMS voltage for one of the cases demonstrates that it is 680.8V, which is lower than expected, while the DC is higher than expected. From the AC voltage, the DC voltage should be $680.8V \cdot 1.35 = 919.08V$.

From the previous simulation, it can be seen that if variable speed operation and droop control are used together, the best simulation results occur when both generators supply the same amount. However, when the two generators supply the same amount of power, there may be some "fighting" between the two generators, leading to instabilities. This is an issue that did not manifest in the simulations here. This may be due to the fact that the model is analytical and therefore does not take into consideration all the different physical aspects of the synchronous generator.

As seen from the case with variable speed operation and droop constants of 0.04 and 0.05, there was little difference between the power supplied by the two generators. The difference between the cases with and without variable speed was extremely large. Therefore, a test was performed for the system with variable speed in which the droop for Generator 1 is increased to 0.1, which means a droop of 10%. Generator 2 had a droop of 5%, which means that Generator 2 should supply an even larger amount of power than it did previously. From the results, it can be seen that now there is a larger difference, but the difference is not as large as it is with the constant speed operation.

6.6 Reasons for instabilities

One reason for the system's instabilities may be that each generator has one variable speed controller. This means that the generators operate at very different speeds considering that Generator 2 supplied much more than Generator 1 in many of the droop cases. From Equation 9b it can be seen that in this analytical model for the synchronous generator, the speed is used to calculate the voltage for the generator. With large differences in speed, the voltage from the generator will also be quite different and this will result in different DC voltage and could be the cause of this instability. Therefore, some tests were conducted in which one generator set the speed for both generators to observe how the system behaves.

The results from Figures 48, 49 and 50 show that when using Generator 2 to set the speed for both generators, the speed of both generators becomes 975RPM. This is due to the fact that the speed is set by Generator 2, which basically produces all the power and will therefore operate at almost maximum speed. The signals are now much better than they were previously. The DC voltage has a much smoother oscillation, while the power has almost no oscillation. This result is quite similar to the result with droop without variable speed operation, which was carried out earlier in the project. The power result is also better compared to previous cases with variable speed operation. However, there is one issue, which is that after the load change, the load is not properly supplied. Generator 2 supplies 2862kW, while Generator 1 supplies 0.024kW. The load should be 3118kW, and this means that the load is not properly supplied. In this case, it would make sense for Generator 1 to supply some power to supplement the power that Generator 2 is not supplying, but this does not happen.

Examining the case in which the speed is controlled by Generator 1, it should be noted that both the power and voltages are similar for both cases. The only difference is that the generators operate at 975RPM when Generator 2 controls the speed and at 500RPM when Generator 1 controls the speed. The fact that the speed for both generators is 500RPM is not realistic since one of them is supplying almost its maximum capacity. Had it not been for the lowest speed in the lookup table being 500RPM, it is likely that the speed would have decreased to zero. Using the highest speed generator would then be the most logical choice, but it would also be strange for the generator that barely supplies any power to run at maximum speed. This was also tested, but the same results were with Generator 2 controlling as they were with Generator 1 controlling except for the speed. This shows that for this model, the speed does not affect the power supplied from the generator. It is not logical that the result is basically the same even though the speed is almost doubled in one case. Therefore, it appears that some defects in the model do not take the speed into consideration.

There is one PI controller and one PID controller for each generator. PI and PID controllers are linear-type controllers, and it is not always easy to ensure the stability of these controllers. Since these are tuned for specific load conditions, they are difficult to optimize for the load sharing [31]. Considering this, some new simulations were created, in which the PI controller as governor was switched with the finished block from Simulink. This governor did not have a PI controller, which could indicate whether the PI controller is one of the issues that leads to the instabilities. Examining the results from the simulations in Figure 54, 55 and 56 it can be observed that the results are better than for the previous cases with variable speed operation. The result is not as good as that with constant speed, but it is better than the other cases with variable speed for each generator. These results show that the PI controller for the governor is one of the reasons for the instability. There are still many oscillations in the power, which is not optimal because this will mean that the power supplied from the generators will change all the time.

6.7 Linear model

The results from the linear model shows that the system is unstable. This can be seen from the eigenvalues in Figure 57. In this case, there are eight eigenvalues and three of them are on the right-hand side of the y-axis. This configuration means that the system is unstable, and to stabilize the system, these eigenvalues need to be moved to the left side of the y-axis. The most similar case in the Simulink model to the linear model is the case in Figure 23. This example is before the diode rectifier and DC load have been implemented and therefore is the most similar. The results from the Simulink model are stable, and therefore it is highly likely that the linear model will also be stable.

Examining at the block diagram for the linear model in Figure 21, it can be observed that it is very similar to the Simulink model for the generator. The excitation system and governor are exactly the same with the same values. The only difference between the two models is that the windings have been taken into account for the linear model. The expression for the field winding and the constant for the armature winding are used in the models on which the linear model is based. Therefore, they have also been included in the linear model for this project. The values for the constants are also the same as the model in [27]. They can also be calculated, but the calculation is not easy to perform due to some missing parameters for the generator. For this reason, the values used in the other model were used in this case, and then they were changed to observe whether there were any changes. On changing the values for the parameters, the system did not become stable; the main change was that the imaginary part of the poles became smaller or larger depending on which values were changed. Since one of the changed parameters is the damping, it would make sense that the imaginary part is smaller since there is less oscillation in the system. This should mean that the parameters are not the main reason for the instability in the linear model.

Another possible reason for the instability in the linear model is the expressions for the armature and field winding. This reason relates mainly to the field winding, considering that it is an expression while the armature winding is just a constant. Perhaps this is something that should be added to the Simulink model to make it more realistic. However, considering the fact that many of the simulations for the Simulink model produce results that make sense, it appears that it is fine without the windings. The model in [27] also has an expression for the turbine, but this part has been removed for the linear model in this project. This expression was removed since the same was done for the Simulink model. The turbine in [27] is also intended to be a water turbine which is not required in this project.

There is also a possibility that there are some faults in the script created for the linear model. However, these faults can be quite hard to detect. Another possibility is that there are some faults in the differential equations for the linear model. The equations were not taken from a particular source, they were simply found using the similar methods to [27], [28] and [29]. This means that there is the possibility of human error within the equations. There is also the possibility of errors occurring in transferring the functions from paper to script. Typographical errors in scripts can have a large influence on the results; however, as long as they run, no message is produced that conveys that the functions are wrongly written.

7 Further work

The project has been heavily focused on simulations, and the possibility exists of utilizing more theory behind the different simulations that were carried out. More cases could also be tested, such as adding more generators to the system to observe how they will react and also adding more components overall.

The only load used for this project was a constant voltage load. The resistance of this load will vary depending on the DC voltage. This may be one of the reasons that the DC voltage is so different in the different cases. More closely investigating the load is a study that could also be undertaken. In the DC grids in ships there are different motors in which other types of loads are supplied. These should be tested to establish whether the model also works for these cases. There is a possibility that the model will not be able to properly simulate loads other than the constant voltage load since this is the simplest type of load. The final goal for the model should be to further increase the model culminating in the total grid system for a ship with several generators and different types of components.

The model is based on an analytical model, which means that some physical occurrences in the real world may not be represented or the model will not act in the same way as the real generator. Factors such as the reactance and also the rotor resistance were not taken into account in this model. All these things will affect the behavior of the generator but are not considered in the analytical model because it is based on a virtual synchronous generator. It can also be quite common for a simplification of the project to not take these factors into considerations. A way to ensure that the results from the model is correct can then be to pair the analytical model with the real generators and then use the these results to verify the analytical model.

From the change in governor model, it was established that the results were better when the governor did not include a PI controller. This may be the same case for the excitation system. The AVR in the excitation system consists of a PID controller and this may be one of the reasons for the "messy" signal. Therefore the excitation system should be changed to another one without a PID or at least the AVR should be changed. Attempts were made to remove the integrator part of the PID and also the whole PID but this resulted in more unstable results and values that were too low. These unstable results indicate that just removing the PID is insufficient; it needs to be replaced by something similar to the governor.

There were some cases where too much power was supplied to the load. This was especially true for the cases with variable speed operation. If too much power is supplied, this will also lead to higher speeds than necessary along with higher costs, and it can also damage the system. Therefore, more control should be implemented to prevent the supply of too much power for both generators. There were cases in which one of the generators supplied power of over 3000kW, which is much higher than the rated power of 2589kVA. Having the generators in the simulation supply much more than they are capable of in real life will not make for simulations which can be properly used in normal operations on board the marine vessels.

The linear model created for the project was not prioritized until late in the project and therefore remains unfinished. There many improvements to be made to this model. First, this model needs to simulate in the same way as the analytical model to obtain a proper comparison between the two models. Since these models are not connected in any way, the linear model can be used to verify the analytical model or vice versa. The linear model can be used not only to verify the results but also to further investigate the stability issue in the variable speed operation with the droop controller. By using the linear model to examine the eigenvalues for the system, it should be possible to determine which eigenvalues are unstable and connect these with different parts of the system to discover where the instability occurs. This will also make it easier to find a solution rather than just changing parts of the analytical model without knowing where the issue is actually occurring.

To date, the linear model is able to calculate the eigenvalues for one generator with the governor and excitation system. There are many further improvements to undertake on the model. The first task, is to make the linear model stable; considering the Simulink model is stable for an AC load, the linear model should also be stable when in operating similar cases. When the linear model is stable, the model should be further developed to operate with a DC load and then to operate in parallel.

It should also be possible to obtain the same values from the linear model as the Simulink simulation. This should be the final step after getting the proper eigenvalues for he the model. Doing so will mean that the values can be plotted together with the values from the Simulink model and used as a comparison. Thus far, the reference values for the voltage and speed are just set as constant 1. In the Simulink model, the reference voltage is decided using droop control when operating in parallel. The same applies to the speed reference, but it is decided using variable speed operation with a look up table depending on the power the generator supplies. This means that new equations need to be created for the reference values, which will not be as simple as before. This may also lead to new inputs and more state variables.

8 Conclusion

In this master's thesis, a Simulink model for a DC grid with two generators operating in parallel to supply the same load was created. This model was created with the goal of operating with variable speed and droop control. An excitation system of the AC8B type is used. For the governor, a PI controller was tested as well as a governor block already created in Simulink.

The first tests for the model were with normal parallel operations for two generators with and with out adding any additional load to the system. When there is no load change, the system operates as expected and supplies the correct load, but with a load change, the power of the load is slightly lower than expected. The results are also very similar to the detailed model.

By using droop control, the generator with the lowest droop constant will supply the most power to the load. The second generator will then supply the rest and also act as a backup to provide the system with more reliability and safety. By increasing and decreasing the droop constant, it is possible to control how much power each generator supplies to the load or how large the voltage drop for each generator will be. On changing the droop constant for Generator 2 to 0.04, Generator 1 supplied less than Generator 2. The system was still stable, but the difference in the supplied power was not as expected. Generator 1 supplies less than expected while Generator 2 supplies more than expected.

Using variable speed operation with synchronous generators is one of the advantages of using a DC grid. This system allows a more fuel efficient operation and is also better for the system. Other advantages of using a DC grid are that the grid is more space efficient and also more cost efficient with less need for transformers and AC filters. Using a lookup table, the reference speed for the generators is changed depending on the power it supplies. Initially testing one generator, the speed regulated well with the power supplied and the system looked stable. After beneficial results with one generator, another generator with variable speed was added to the system. The system was still stable, but both the power and DC voltage were too high. Both generators operated at the same speed, as there was no droop control so they supplied the same amount of power.

When operating with droop control and variable speed for two generators in parallel, some instability occurs. There is also much less difference between how much power the two generators supply. To actually determine which generator supplies the most power, there needs to be larger difference than 0.01 between the droop constants. One of the reasons for this instability is the fact that the control systems have PID elements. It is difficult to ensure stability for these components and this can lead to instability for the system. By changing the PID elements, the system will become more stable. The system is stable as long as the droop control or variable speed is used separately, but when they are used at the same time, the instability occurs.

One solution to prevent the instabilities from occurring is to have both generators operating at the same speed. This can be achieved by using variable speed operation for one of the generators and using this to control the speed of the other generator. In this case, the most logical choice would be to use the generator that supplies the most power to control the speed of both generators.

Using a linear model of a system provides an opportunity to look further into the stability of the system and also makes it easier to notice instabilities. A linear model that is made correctly can also be used to simulate similar cases to the generators out in the field. The linear model control system and generator gave eight eigenvalues with three on the right-hand side of the y-axis. This configuration indicates that the model is unstable and requires further improvements.

Appendices

A Acronyms

DC Direct current

LVDC Low voltage direct current

AC Alternating current

pu Per unit

PID Proportional Integral Derivative

kW Kilo watts

kJ Kilo joule

kWh Kilo watts hour

RPM Revolutions per minute

B Tables

Table 2: Values for the synchronous generator

Parameter	Value	Comment
P_{mech_N}	2430kW	Nominal mechanical power
P_{e_N}	2330kW	Nominal electrical power ($\cos(\phi) = 0.9$)
τ_N	23205Nm	Nominal mechanical shaft power output at ω_n
f_N	50Hz	Nominal frequency
$\cos\phi_N$	0.9	Nominal power factor
n_N	1000rpm	speed
V_{base}	705V	Nominal voltage
I_N	2120.2A	Nominal current
S_{base}	2589kVA	Base power
Zs_{base}	0.192Ohm	Base impedance
w_{ref}	$2*\pi*50$	Reference speed
Tm	2770Nm	Mechanical torque
M	430kgm^2	Inertia
D	2.47	Damping coefficient
pp	3	Pole pairs
T_d’	0.364s	Transient time constant (short circuit)
T_d"	0.014	Subtransient time constant (short circuit)
T_{d0}’	3.141s	Transient time constant (open circuit)
T_{d0}"	0.024s	Subtransient time constant (open circuit)
K_2	0.7	Field winding linearization constant
K_3	0.5	Field winding linearization constant
K_6	0.4	Armature winding linearization constant
$K_{E'}$	2.15	Linearization constant for synchronizing power [pu]
D_δ	1.05	Linearization constant [pu]
V_{ref}	1	Reference voltage [pu]
ω_{ref}	1	Reference speed [pu]

Table 3: Values for the excitation system

Parameter	Value	Comment
K_A	2.4pu	Regulator gain
T_A	0.15s	Regulator time constant
V_{Rmax}	7.75pu	Maximum output voltage
V_{Rmin}	0pu	Minimum output voltage
SAT	0.153pu	Saturation curve constant
K_{E_070}	0.12pu	Exciter gain at 700rpm
K_{E_100}	0.2pu	Exciter gain at 1000rpm
K_{E_m}	1.667pu	Exciter gain slope from 700 to 1000rpm
T_E	0.151s	Exciter time constant
T_α	3.292s	Sum of large time constants
T_{fv}	0.4938s	Voltage measurment filter assuming 2% ripple
K_{sv}	0.2880	OMC constant
T_β	3.7858	OMC sum of parasitic time constants
K_P	4.5290	AVR proportional gain
K_I	1.3758	AVR integral gain
K_D	5	AVR derivative gain
T_D	2s	AVR derivative time constant

Table 4: Values for governor

Parameter	Value	Comment
T_{fw}	1.11e-5s	Filter time constant
K_{PW}	100	P governor
K_{IW}	896	I governor

C Matlab script for analytical model

```
Ts = 2e-5;

%Rated nominal values:
P_mech_N = 2430e3;%[W]
P_e_N = 2330e3;%[W] Nominal electric power output at cos(phi) = 0.9
tau_N = 23205;%[Nm] Nominal mech. shaft power output @ W_N
f_N = 50; %Hz
cos_phi_N = 0.9;% Nominal power factor
n_N = 1000;%[rpm] Speed

%Base values
V_N = 705*sqrt(2);%[V]
I_N = 2120.2;%[A]
S_base = 2589e3;%[VA]
Is_base = I_N;%[A] from 35-50[Hz]
Vs_base = V_N/sqrt(3);%[V] approx. 407.044[V]
Zs_base = 0.192;%[Ohm]
W_base = 2*pi*f_N;%[rad/s]
Ls_base = Zs_base/W_base;%[H]

R_s = 0.007145833;%[pu] Stator resistance
L_s = 0.005; %Random value to test
R_r = 1.485;%[Ohm] Rotor resistance
Tm = 2470;
J = 430;
D = 2.47;
w_ref = 2*pi*50;
wind = 6; %windings
```

```
x_d = 1.532;%[pu] Steady state reactances (d- and q-axis)
x_q = 0.674;%[pu]

x_d_tr = 0.161;%[pu] Transient reactances (d- and q-axis)
x_q_tr = 0.674;%[pu]

x_d_subtr = 0.106;%[pu] Sub-transient reactances (d- and q-axis)
x_q_subtr = 0.113;%[pu]

% Speed-constraints
    n_max = 1000;%[rpm] Maximum mech. speed

% Number of cylinders
    Nc = 9;

% Mech.const.
    J_m = 265.59;%[kgm^2] Machine + mech. coupling

 J_g = 430;%[kgm^2] Mechanical inertia
    pp = 3;% Pole pairs
    H = ((J_g+J_m)*(n_N*(pi/30))^2)/(2*S_base);%[s] Inertia constant
% Gain constant:
    P_SI = P_mech_N/P_e_N;

%   Armature time constant
    T_a = 0.044;%[s] Armature time constant
```

```
%   Direct axis open circuit:
    T_d0_tr = 3.141;%[s] Transient open circuit time constant
    T_d0_subtr = 0.024;%[s] Subtransient open circuit time constant

%   Quadrature axis open circuit:
    T_q0_tr = 0.180;%[s] Transient open circuit time constant
    T_q0_subtr = 0.155;%[s] Subtransient open circuit time constant

%   Direct axis short circuit:
    T_d_tr = 0.364;%[s] Transient short circuit time constant
    T_d_subtr = 0.014;%[s] Subtransient short circuit time constant

%   Quadrature axis short circuit:
    T_q_tr = 0.180;%[s] Transient short circuit time constant
    T_q_subtr = 0.018;%[s] Subtransient short circuit time constant

% Voltage regulator:
K_A = 2.4;%[pu] Regulator gain (arbitrary standard value of AC2A)
T_A = 0.15;%[s] Regulator time constant (arbitrary standard value of AC2A)
V_Rmax = 7.75;%[pu] Maximum output voltage
V_Rmin = 0;%[pu] Minimum output voltage

% Excitation system:
SAT = 0.153;%[-] Saturation curve constant
K_E_070 = 0.12;%[pu] Exciter gain at 700[rpm]
K_E_100 = 0.2;%[pu] Exciter gain at 1000[rpm]
K_E_m = K_E_100/K_E_070;%[-] Exciter gain slope (from 700-1000[rpm])
T_E = 0.151;%[s] Exciter time constant
```

```
T_iv = T_d0_tr+T_E;%[]
T_fv = 0.15*T_iv;%[s] Voltage measurment filter assuming 2% ripple
K_sv = K_A*K_E_070;%[-] OMC constant
T_sumv = T_iv+T_fv;%[s] OMC sum of parasitic time constants

% AVR PID parameters
K_P = 3*(T_iv/(2*K_sv*T_sumv));%[-] P gain (manual tuning yields 3*K_PR0)
K_I = 1*(K_P/T_iv);%[-]
K_D = 5;%[-] D gain (Manually tuned)
T_D = 2;%[s] D time coonstant (Manually tuned)

%Governor parameters
T1 = 0.01;
T2 = 0.02;
T3 = 0.2;
K = 40;
T4 = 0.25;
T5 = 0.09;
T6 = 0.0384;
T_delay = 0.024;
T_max = 1.1;
T_min = 0;
```

```
%Governor
% The speed controller is modelled as a simple PI controller using 'Optimum
% Symmetric' criterion with a dynamic reference speed setpoint.
% The inner loop is regarded as a first order delay, i.e., T_eqtau.
%
T_fw = 1.11e-5;
K_pw = 100;%[-] Proportional gain (manually tuned)
K_iw = 896;%[-] Integral gain (Cacluated from symmetrical optimum


% AVR power control variables
K_vdc = 0.05;%[pu] DC voltage droop at 5%
V_ref_DC = 1.0388;%[pu] DC voltage reference (larger than one due to steady
% state error when V_ref_DC = 1.00)
```

References

[1] Espen Skjong et al. "The Marine Vessel's Electrical Power System: From its Birth to Present Day". en. In: *Proceedings of the IEEE* 103.12 (Dec. 2015), pp. 2410–2424. ISSN: 0018-9219, 1558-2256. DOI: 10.1109/JPROC.2015.2496722. URL: http://ieeexplore.ieee.org/document/7329674/ (visited on 05/09/2021).

[2] Kyunghwa Kim et al. "DC-grid system for ships: a study of benefits and technical considerations". en. In: *Journal of International Maritime Safety, Environmental Affairs, and Shipping* 2.1 (Nov. 2018), pp. 1–12. ISSN: 2572-5084. DOI: 10.1080/25725084.2018.1490239. URL: https://www.tandfonline.com/doi/full/10.1080/25725084.2018.1490239 (visited on 05/08/2021).

[3] *Shipping 4.0 - Onboard DC Grid - a system platform at the heart of Shipping 4.0*. en. URL: https://new.abb.com/marine/generations/generations-2017/business-articles/onboard-dc-grid-a-system-platform-at-the-heart-of-shipping (visited on 05/08/2021).

[4] Tomas Skaar Vadset. *Analytical model for a synchronous generator*. Dec. 2020. (Visited on 01/13/2021).

[5] *MATLAB - MathWorks*. en. URL: https://se.mathworks.com/products/matlab.html (visited on 05/08/2021).

[6] *Simulink - Simulation and Model-Based Design*. en. URL: https://se.mathworks.com/products/simulink.html (visited on 05/08/2021).

[7] *Simscape Electrical*. en. URL: https://se.mathworks.com/products/simscape-electrical.html (visited on 05/08/2021).

[8] Roy Nilsen and Ingve Sorfonn. "Hybrid Power Generation Systems". In: *2009 13th European Conference on Power Electronics and Applications*. Sept. 2009, pp. 1–9.

[9] Hyeonmin Jeon and Jongsu Kim. "Application of Reference Voltage Control Method of the Generator Using a Neural Network in Variable Speed Synchronous Generation System of DC Distribution for Ships". en. In: *Journal of Marine Science and Engineering* 8.10 (Oct. 2020). Number: 10 Publisher: Multidisciplinary Digital Publishing Institute, p. 802. DOI:

10.3390/jmse8100802. URL: https://www.mdpi.com/2077-1312/8/10/802 (visited on 04/21/2021).

[10] Bijan Zahedi and Lars Einar Norum. "Voltage regulation and power sharing control in ship LVDC power distribution systems". In: *2013 15th European Conference on Power Electronics and Applications (EPE)*. Sept. 2013, pp. 1–8. DOI: 10.1109/EPE.2013.6631763.

[11] Jinxin Zhao and Florian Dörfler. "Distributed control, load sharing, and dispatch in DC microgrids". In: *2015 American Control Conference (ACC)*. ISSN: 2378-5861. July 2015, pp. 3304–3309. DOI: 10.1109/ACC.2015.7171842.

[12] Tron Hansen Syverud. *Modeling and Control of a DC-grid Hybrid Power System with Battery and Variable Speed Diesel Generators*. June 2016. (Visited on 02/22/2021).

[13] *What is Automatic Voltage Regulator? Meaning, Working Principle & Applications*. en-US. Aug. 2016. URL: https://circuitglobe.com/automatic-voltage-regulator.html (visited on 05/08/2021).

[14] Daniel Gray. *(7) overfluxing*. URL: https://www.slideshare.net/DanielGray11/7-overfluxing (visited on 04/18/2021).

[15] *The Advantages of Variable Speed Gensets*. en. July 2020. URL: https://www.marinelink.com/news/advantages-variable-speed-gensets-480588 (visited on 03/02/2021).

[16] Jan Fredrik Hansen, John O Lindtjørn, and Klaus Vanska. "Onboard DC Grid for enhanced DP operation in ships". en. In: (2011), p. 8.

[17] Eleftherios Dedes, Dominic Hudson, and Stephen Turnock. "Assessing the potential of hybrid energy technology to reduce exhaust emissions from global shipping". In: *Energy Policy - ENERG POLICY* 40 (Jan. 2011). DOI: 10.1016/j.enpol.2011.09.046.

[18] Preben Sandve Solvang. "State Space Model Based PID Controller Tuning". en. In: (), p. 171.

[19] J Slootweg et al. "A study of the eigenvalue analysis capabilities of power system dynamics simulation software". In: (June 2002).

[20] Jan Machowski, Janusz W. Bialek, and James R. Bumby. *Power System Stability and Control*. Second. 1. John Wiley & Sons, Ltd. ISBN: 978-0-470-72558-0.

[21] Prabha Kundur. *Power System Stability and Control*. en-US. McGraw-Hill, Inc., 1993. ISBN: 0-07-035958-X.

[22] *Perform transformation from three-phase (abc) signal to dq0 rotating reference frame or the inverse - Simulink - MathWorks Nordic*. URL: https://se.mathworks.com/help/physmod/sps/powersys/ref/abctodq0dq0toabc.html?s_tid=doc_ta (visited on 05/10/2021).

[23] Qing-Chang Zhong and George Weiss. "Synchronverters: Inverters That Mimic Synchronous Generators". In: *IEEE Transactions on Industrial Electronics* 58.4 (Apr. 2011). Conference Name: IEEE Transactions on Industrial Electronics, pp. 1259–1267. ISSN: 1557-9948. DOI: 10.1109/TIE.2010.2048839.

[24] *Difference Between Diode and Thyristor (with Comparison Chart)*. en-US. June 2019. URL: https://circuitglobe.com/difference-between-diode-and-thyristor.html (visited on 04/25/2021).

[25] Salvatore D'Arco. *ELK-23: Power Electronics in Future Power Systems, Control system Design and tuning for voltage source converterrs*. 2020. (Visited on 04/25/2021).

[26] Roy Nilsen. *TET4120 Electric drives compendium*. 2016. (Visited on 04/25/2021).

[27] Mohammad Amin. *TET4180 - Power System Stability and Control, Exam soulution 2020*. en. June 2020.

[28] Mohammad Amin. *TET4180 – Power System Stability and Control, Slides :Chapter 6: Electromechanical Dynamics – Small Disturbances*. Jan. 2020.

[29] Mohammad Amin. *TET4180 – Power System Stability and Control, Slides: Chapter 5: Electromechanical Dynamics – Small Disturbances (2)*. Jan. 2020.

[30] "IEEE Recommended Practice for Excitation System Models for Power System Stability Studies". In: *IEEE Std 421.5-2016 (Revision of IEEE Std 421.5-2005)* (Aug. 2016). Conference Name: IEEE Std 421.5-2016 (Revision of IEEE Std 421.5-2005), pp. 1–207. DOI: 10.1109/IEEESTD.2016.7553421.

[31] Muhammad Rashad et al. “Proportional Load Sharing and Stability of DC Microgrid with Distributed Architecture Using SM Controller”. en. In: *Mathematical Problems in Engineering* 2018 (2018), pp. 1–16. ISSN: 1024-123X, 1563-5147. DOI: 10.1155/2018/2717129. URL: https://www.hindawi.com/journals/mpe/2018/2717129/ (visited on 04/21/2021).

NTNU

Norwegian University of
Science and Technology